Quaternary Research

doi:10.1017/qua.2020.87

Bone histology, palaeobiology, and early diagenetic history of extinct equids from Turkey

Carmen Nacarino-Meneses[a]*, Anusuya Chinsamy[a], Serdar Mayda[b,c], Tanju Kaya[c], Ugur Cengiz Erismis[d]

[a]University of Cape Town, Department of Biological Sciences, Private Bag X3, Rhodes Gift, Cape Town, 7700 South Africa
[b]Ege University, Faculty of Science, Biology Department, Bornova, Izmir, 35100 Turkey
[c]Ege University, Natural History Museum, Bornova, Izmir, 35100 Turkey
[d]Afyon Kocatepe University, Faculty of Science and Literature, Molecular Biology and Genetics Department, Afyonkarahisar, 03200 Turkey
*Corresponding author at: E-mail address: carmen.nacarino@gmail.com (C. Nacarino-Meneses).

(Received March 27, 2020; Accepted August 25, 2020)

Abstract

Bone histology has proved to be a valuable tool to obtain information about the palaeobiology and early taphonomic history of fossil vertebrates. However, there are still many extinct taxa for which bone histology studies could be applied to deduce information about their life history and early diagenetic changes. Here, we partially fill this gap by studying bone microstructure and bone micropreservation in the third metapodia of *Hipparion* and *Equus* recovered from several Miocene, Pliocene, and Pleistocene localities in Turkey. Our histological analysis reveals that most of the bone cortices under study are composed of a well-vascularized fibrolamellar bone. Furthermore, we record the presence of compact coarse cancellous bone in a *Hipparion* metatarsal. In terms of histological preservation, our findings provide supporting evidence that differences in moisture, oxygen, and/or temperature during fossilisation at the different localities impacted the quality of bone preservation. Bacterial bioerosion was extensive in the samples, and we also identified a specific tunnelling morphology that we tentatively consider to be damage caused by freshwater algae. The present study provides novel insight into the palaeobiology and early diagenetic history of extinct horses from Turkey and sets the stage for further research in this area.

Keywords: Equidae; Bone histology; Palaeobiology; Skeletochronology; Bioerosion; Diagenesis

INTRODUCTION

Horses (i.e., family Equidae) are key taxa in palaeontological and evolutionary studies due to their abundance and widespread presence in the fossil record (MacFadden, 1992, 2005; Orlando, 2015). Among the different equid lineages, Hipparionini and Equini tribes have traditionally received much interest because of their importance as stratigraphical, biochronological, and palaeoecological markers (Strömberg, 2006; van Asperen, 2012; Bernor et al., 2017; Boulbes and van Asperen, 2019; Rook et al., 2019). Turkey has an excellent palaeontological record of both Hipparionini and Equini equids (Tekkaya et al., 1975; Koufos and Kostopoulos, 1994; Forsten and Kaya, 1995; Eisenmann and Sondaar, 1998; Kaya and Forsten, 1999; Geraads et al., 2002; Saraç et al., 2002; Bernor et al., 2003; Kaya et al., 2005a, 2005b, 2012; Koufos and Vlachou, 2005; Mayda et al., 2015). However, most of the studies performed so far on Miocene and Pleistocene Turkish horses have focused on the taxonomy and systematics of the different species (e.g., Kaya et al., 2012), whereas palaeobiological and diagenetic aspects still remain poorly explored.

Bone histology has proved to be a valuable tool for inferring palaeobiological and taphonomic information of prehistoric animals (e.g., Chinsamy-Turan, 2005; Turner-Walker, 2008; Kendall et al., 2018). Despite the host of information that bone histology is able to provide for archaeological and palaeontological vertebrates, it is still not widely addressed in these fields. On the one hand, histotaphonomical works have traditionally focused on archaeological material (e.g., Jans, 2005), and only a few studies thoroughly reported microscopic alterations in the bone tissue of palaeontological samples (Davis, 1997; Trueman and Martill, 2002; Chinsamy-Turan, 2005; Chinsamy-Turan and Ray, 2012; Turner-Walker, 2012; van der Sluis et al., 2014; Tomassini et al., 2015; Lyras et al., 2019; Mayer et al., 2020). Conversely, histological studies on palaeontological

Cite this article: Nacarino-Meneses, C., Chinsamy, A., Mayda, S., Kaya, T., Erismis, U. C. 2021. Bone histology, palaeobiology, and early diagenetic history of extinct equids from Turkey. *Quaternary Research* 100, 240–259. https://doi.org/10.1017/qua.2020.87

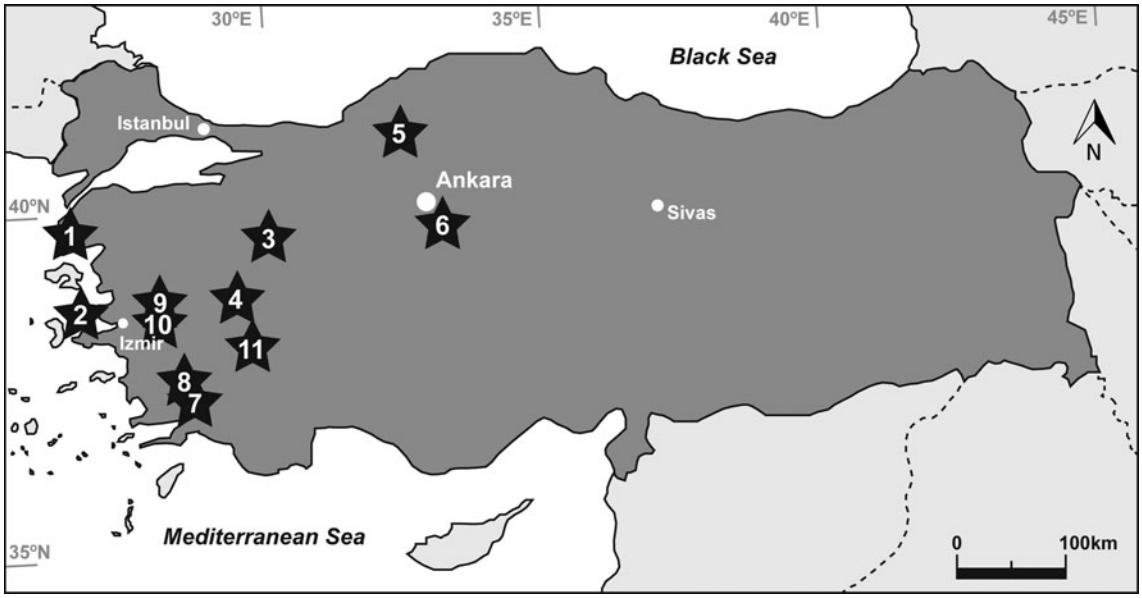

Figure 1. Map of Turkey (dark grey) showing the locations of the localities from which the studied metapodia were recovered: (1) Çanakkale-Gülpınar, (2) Izmir-Karaburun, (3) Kütahya-Bayat, (4) Uşak-Kemiklitepe, (5) Çankırı-Yeniköy, (6) Kırşehir-Kaman, (7) Muğla-Yatağan-Salihpaşalar, (8) Muğla-Yatağan-Şerefköy, (9) Manisa-Düzpınar, (10) Manisa-Aşağıçobanisa, (11) Denizli-Pamukkale. Stars indicate fossil localities and circles depict main cities.

bones have generally aimed at inferring life history information of extinct species (Chinsamy-Turan, 2005; Kolb et al., 2015b), an approach less investigated within archaeological material.

In this paper, we apply bone histology to several *Equus* and *Hipparion* specimens from the Miocene, Mio-Pliocene, and Pleistocene deposits of Turkey (Fig. 1, Table 1) with the objective of describing the bone histology and the microscopic diagenetic alterations of the samples. The main aims of our research are (1) to expand our knowledge of the palaeobiology of extinct equid species and (2) to shed light on the early taphonomic history of the fossils from 11 different Turkish localities.

BACKGROUND

Hipparion and *Equus* palaeontology

Hipparionine horses are characterized by having three-toed limbs and isolated protocones in their upper cheek teeth (Christol, 1832; Alberdi, 1989; Bernor et al., 1990). Originating in the Miocene of North America (MacFadden, 1984, 1985), they reached the Old World around 11 Ma (million years ago) during the migratory event usually referred to as "*Hipparion* datum" (*Cormohipparion* datum after Bernor et al., 2017) (Bernor et al., 1988; Sen, 1990; Garcés et al., 1997). Hipparionine taxa flourished in this continent during Vallesian (European Land Mammal Age, 11.2–8.9 Ma [Hilgen et al., 2012]) and Turolian (European Land Mammal Age, 8.9–5.3 Ma [Hilgen et al., 2012]) periods (Forsten, 1989) and finally became extinct in Europe at the middle Villafranchian (early Pleistocene, 2.6–2.0 Ma [Rook et al., 2019]) (Pueyo et al., 2016). During this latest period, they may have coexisted (Pueyo et al., 2016; Rook et al., 2017) with the only Equini representative distributed worldwide (Prado and Alberdi, 1996): the genus *Equus*, which comprises all living and extinct species of monodactyl horses with extremely hypsodont teeth (MacFadden, 1992). *Equus* first emerged in North America 4–4.5 Ma (Orlando et al., 2013), and thereafter they dispersed to Eurasia (Rook et al., 2019) in two different migration waves (Alberdi and Bonadonna, 1988; Forsten, 1988; Azzaroli, 1992; Alberdi and Cerdeño, 2003). A first dispersal event introduced the stenonid horses (zebras and asses) to Eurasia (Alberdi and Bonadonna, 1988; Alberdi et al., 1998) 3.0–2.5 Ma (*Equus*-Elephant event, Lindsay et al., 1980). Caballoid equids (horses), on the other hand, arrived in Eurasia during a second migration wave that took place in the middle Pleistocene (1–0.8 Ma) (Alberdi and Bonadonna, 1988; Forsten, 1988; Orlando, 2015).

Hipparion s.l. (see Material Section for further explanations on hipparionine taxonomy) and *Equus* are common element faunas in the Neogene and Quaternary of Turkey. From the early Vallesian (MN9 European Land Mammal Age, 11.2–9.9 Ma [Hilgen et al., 2012]) to the early Ruscinian (MN14 European Land Mammal Age, 5.3–5.0 Ma [Hilgen et al., 2012]), Anatolia was inhabited by a high taxonomic diversity of hipparionines, including small-bodied forms (e.g., *H. matthewi*), medium-sized taxa (e.g., *H. dietrichi*), and large-bodied species (e.g., *H. brachypus*) (Tekkaya et al., 1975; Koufos and Kostopoulos, 1994; Forsten and Kaya, 1995; Eisenmann and Sondaar, 1998; Kaya and Forsten, 1999; Geraads et al., 2002; Saraç et al., 2002; Bernor et al., 2003; Kaya et al., 2005a, 2005b, 2012; Koufos and

https://doi.org/10.1017/qua.2020.87 Published online by Cambridge University Press

Table 1. *Hipparion* and *Equus* samples studied. ELMA = European Land Mammal Ages, based on Hilgen and colleagues (2012); MN = European Mammal Neogene Units; Ma = million years ago; Mt-III = third metatarsal; Mc-III = third metacarpal.

Locality	Latitude (°N)	Longitude (°E)	Epoch	ELMA			Taxon	Skeletal element	Specimen
				Age	MN	Date ranges (Ma)			
Çanakkale-Gülpınar	39° 31′ 48″	26° 5′ 24″	Late Miocene	Turolian	MN11-12	11.2–7.4/6.8	*Hipparion*	Mt-III	CG-1
								Mt-III	CG-2
								Mt-III	CG-3
Izmir-Karaburun	38° 36′ 36″	26° 33′ 36″	Late Miocene	Turolian	MN11-12	11.2–7.4/6.8	*Hipparion*	Mt-III	IKE-1
Kütahya-Bayat	39° 20′ 24″	29° 49′ 12″	Late Miocene	Turolian	MN11-12	11.2–7.4/6.8	*Hipparion*	Mt-III	KB-1
Uşak-Kemiklitepe 2	38° 24′ 00″	29° 09′ 00″	Late Miocene	Turolian	MN11-12	11.2–7.4/6.8	*Hipparion*	Mc-III	UEK-1
Çankırı-Yeniköy	-	-	Late Miocene	Turolian	MN11-12	11.2–7.4/6.8	*Hipparion*	Mt-III	CY-1
Kırşehir-Kaman	39° 27′ 36″	33° 33′ 36″	Late Miocene	Turolian	MN12	7.6–7.4/6.8	*Hipparion*	Mt-III	KK-1
Muğla-Yatağan-Salihpaşalar 1	37° 15′ 00″	28° 15′ 36″	Late Miocene	Turolian	MN12	7.6–7.4/6.8	*Hipparion*	Mt-III	MYSA-1
Muğla-Yatağan-Şerefköy	37° 21′ 36″	28° 13′ 48″	Late Miocene	Turolian	MN12	7.6–7.4/6.8	*Hipparion*	Mt-III	MYSE-1
								Mt-III	MYSE-2
Manisa-Düzpınar	38° 40′ 48″	27° 39′ 00″	Miocene–Pliocene	Turolian-Ruscinian	MN13-14	7.4/6.8–5.0	*Hipparion*	Mc-III	MD-7
Manisa-Aşağıçobanisa	38° 33′ 00″	27° 34′ 12″	Early Pleistocene	Villafranchian	MN17	2.5–2.0/1.8	*Equus*	Mt-III	TA-1
Denizli-Pamukkale	37° 52′ 12″	29° 20′ 24″	Early Pleistocene	Villafranchian	MN17-18	2.5–0.6	*Equus*	Mc-III	P-1

Vlachou, 2005; Mayda et al., 2015). Quaternary mammals from Turkey are less studied (Erten et al., 2005) than late Miocene ones (Demirel and Mayda, 2014), but still different stenonid *Equus* have been described in Plio-Pleistocene and early Pleistocene deposits (Kostopoulos and Sen, 1999; Alçiçek et al., 2012; Mayda et al., 2013; Demirel and Mayda, 2014; Lebatard et al., 2014; Rausch et al., 2019).

Studies on bone histology

Since the seminal works of Enlow and Brown (Enlow and Brown, 1956, 1957, 1958) and de Ricqlès (e.g., de Ricqlès, 1975), numerous authors have analysed the bone microstructure of extinct vertebrates to reconstruct different aspects of their life history (e.g., Chinsamy-Turan 2005). These inferences of extinct taxa rely on our understanding of the histology of extant species (e.g., Köhler et al., 2012), which has shown that key life history traits like birth, growth rate, age at maturity, and age at death are recorded in the bone microstructure (Amprino, 1947; Chinsamy et al., 1995; de Margerie et al., 2002; Castanet et al., 2004; Chinsamy and Valenzuela, 2008; Erismis and Chinsamy, 2010; Marín-Moratalla et al., 2013; Kolb et al., 2015b; Jordana et al., 2016; Nacarino-Meneses et al., 2016a; Montoya-Sanhueza and Chinsamy, 2017; Nacarino-Meneses and Köhler, 2018). In extinct mammals, palaeohistological investigations have focussed on bones of extinct rodents (Geiger et al., 2013; Kolb et al., 2015b; Orlandi-Oliveras et al., 2016; Garrone et al., 2019; Miszkiewicz et al., 2019, 2020), lagomorphs (Kolb et al., 2015b; Moncunill-Solé et al., 2016), hedgehogs (Kolb et al., 2015b), wombats (Walker et al., 2020), hippos (Kolb et al., 2015b), seals (Woolley et al., 2019), bovids (Köhler and Moyà-Solà, 2009; Marín-Moratalla et al., 2011), cervids (Amson et al., 2015; Kolb et al., 2015a; Lyras et al., 2016, 2019), ursids (Veitschegger et al., 2018), and equids (Sander and Andrássy, 2006; Martínez-Maza et al., 2014; Orlandi-Oliveras et al., 2018; Nacarino-Meneses and Orlandi-Oliveras, 2019; Zedda et al., 2020).

Bone histology also provides relevant insights into the early taphonomic history of fossil samples (Garland, 1989; Child, 1995; Pfretzschner, 2004; Jans, 2005, 2008; Turner-Walker, 2008; Pfretzschner and Tütken, 2011; Kendall et al., 2018). In 1864, Wedl described some small tunnels boring the microstructure of ancient bones and tentatively identified fungi, microscopic parasites, and/or parasitic plants as the cause (Turner-Walker, 2008, 2019). Since this pioneering work, different experiments have related the presence, shape, and size of these microscopic foci to the diagenetic action of several microorganisms (Marchiafava et al., 1974; Hackett, 1981; Fernández-Jalvo et al., 2010; Fernández-Jalvo and Andrews, 2016; Pesquero et al., 2018; Turner-Walker, 2019). Today, it is well known that aerobic bacteria (Hackett, 1981; Kendall et al., 2018; Turner-Walker, 2019), cyanobacteria (Davis, 1997; Turner-Walker and Jans, 2008; Turner-Walker, 2012), and algae (Davis, 1997; Fernández-Jalvo et al., 2010) are important bioerosion agents that

https://doi.org/10.1017/qua.2020.87 Published online by Cambridge University Press

leave permanent marks on the bone tissue (Jans, 2008), while the role of fungi as bone tunnellers (Marchiafava et al., 1974) is still under debate (Fernández-Jalvo and Andrews, 2016; Turner-Walker, 2019). The action of microorganisms is affected by different environmental factors, including water, soil pH, or temperature (Child, 1995; Nielsen-Marsh et al., 2000; Hedges, 2002; Kendall et al., 2018; Turner-Walker, 2019). Some of these abiotic factors, like water or temperature, can further produce microcracks in the bone tissue during fossilization (Pfretzschner, 2000, 2004; Jans, 2005; Pfretzschner and Tütken, 2011). Thus, the histo-taphonomical analysis of fossil bones can yield important information about the physical factors affecting their depositional environments (Pfretzschner and Tütken, 2011; Dal Sasso et al., 2014). Moreover, microscopic bioerosion influences the long-term survival of bones in the fossil record, as well as the quantity and quality of the biological information recorded on them (Child, 1995; Trueman and Martill, 2002; Galligani et al., 2019; Turner-Walker, 2019).

MATERIAL AND METHODS

Material

We studied 14 *Hipparion* and *Equus* fossil metapodia recovered from various late Miocene, Mio-Pliocene, and early Pleistocene localities spread across the west of Turkey (see Fig. 1, Table 1). Specifically, metatarsi III (henceforth metatarsi) and metacarpi III (henceforth metacarpi) were the bones selected for the study, as these are the most common skeletal elements of equids found in palaeontological sites.

Systematics and phylogeny of Old World hipparionines is still unclear: Woodburne and Bernor (1980) suggest that, considering the taxonomic variability of this group, all taxa should be grouped at a supra-specific level (e.g., *Cremohipparion*, *Hippotherium*), while Alberdi (1989) argues that the taxa should be classified into different morphotypes all belonging to the genus *Hipparion* s.l. Due to the fragmentary condition of the bones analysed here, we use *Hipparion* as a generic name for the different hipparionine samples under study. We will only refer to other hipparionine genera (i.e., *Cremohipparion*, *Hippotherium,* etc.) to maintain the original taxonomy used in previous investigations (1) when describing the different fossil sites and (2) when making palaeobiological inferences if only one hipparionine species was reported at a specific fossil site.

Çanakkale-Gülpınar

We analysed three metatarsi from the Çanakkale-Gülpınar fossil site (see Table 1). This Turolian locality (MN11-12, 11.2–7.4/6.8 Ma [Hilgen et al., 2012]) (Koufos et al., 2018) is a seashore cliff 3 km southwest of the city of Gülpınar (Çanakkale province) (Forsten and Kaya, 1995) (see Fig. 1). Fossil bones were collected from a fluvial sedimentary sequence that includes brownish sandy and limy mudstones, limestones, sandstones, and conglomerates (Forsten and Kaya, 1995). A variety of large mammals were found in this locality, including both carnivores (Koufos et al., 2018) and herbivores (Forsten and Kaya, 1995). Regarding equids, Forsten and Kaya (1995) described three different *Hipparion* morphotypes: *H*. cf. *matthewi* (small-sized), *H*. sp. medium-sized, *H*. sp. large-sized.

Izmir-Karaburun

One metatarsus from the early Turolian (MN11-12 11.2–7.4/6.8 Ma [Hilgen et al., 2012]) fossil locality of Izmir-Karaburun (Kaya et al., 2005a) is included in this study (see Table 1). It belongs to the so-called Esendere fauna from the Esendere locality, in the Karaburun Peninsula, west of Izmir (Kaya et al., 2005a) (see Fig. 1). Specifically, fossil bones were recovered from the upper part of the Karaburun Formation, a muddy fluvial assemblage grading upwards into lacustrine facies (Kaya, 1981; Kaya et al., 2005a). The geology of the area mainly consists of massive mudstone and lithic sandstone, with oolitic limestone, claystone, and conglomerate occurring subordinately (Kaya et al., 2005a). The Esendere fauna is significant because of the description of two new carnivore species (Kaya et al., 2005a). Other mammalian taxa such as *Cremohipparion* cf. *mediterraneum* were also found in this locality (Kaya et al., 2005a).

Kütahya-Bayat

One metatarsus from Kütahya-Bayat locality was analysed (see Table 1). Fossil mammalian remains at this fossil-bearing site were recovered from the alluvial channel deposits filled with reddish conglomerates, brownish claystone, and mudstone of the Çokköy Formation in Bayat village, 40 km southwest of Kütahya (Kütahya province) (see Fig. 1) (Kaya et al., 2005b). The Bayat faunal assemblage is characterized by the presence of different herbivores, among which the hipparionine species *Cremohipparion* cf. *matthewi* and *Cremohipparion* cf. *mediterraneum* are outstanding (Kaya et al., 2005b). The characteristics of these and other mammalian species indicate a late Miocene age for the site (Turolian, MN11-12, 11.2–7.4/6.8 Ma [Hilgen et al., 2012]) (Kaya et al., 2005b).

Uşak-Kemiklitepe 2

We analysed one metacarpus from the Uşak-Kemiklitepe 2 Turolian locality (MN11-12, 11.2–7.4/6.8 Ma [Hilgen et al., 2012]) (see Table 1). This fossiliferous site is located 1.5 km south of Karacaahmet village (Uşak province) (Sen et al., 1994) (see Fig. 1) in the Asartepe Formation (Seyitoğlu et al., 2009). Specifically, fossils were collected from a clastic unit composed of massive mudstones that alternate with matrix-supported fine-grained conglomerates representing subaerial deposition in distal alluvial-fan environments (Seyitoğlu et al., 2009). Equidae specimens from this locality were

https://doi.org/10.1017/qua.2020.87 Published online by Cambridge University Press

studied by Koufos and Kostopoulos (1994), who described *Hipparion mediterraneum*, *Hipparion matthewi*, and a large-size *Hipparion* sp.

Çankırı-Yeniköy

One metatarsus from the fossiliferous locality of Çankırı-Yeniköy was analysed (see Table 1). This fossil-bearing site is located in the red beds around Yeniköy (Çankırı province) (Sen et al., 1998) (see Fig. 1). The geology of the area is characterized by the presence of alternating sandstones, siltstones, mudstones, and gypsum that represent an alluvial flood plain depositional environment with braided stream channels (Tekkaya et al., 1975). Tekkaya and colleagues (1975) provided a faunal list that includes the presence of *Hipparion gracile*, which suggests a Turolian age (MN11-12, 11.2–7.4/6.8 Ma [Hilgen et al., 2012]) for this locality.

Kırşehir-Kaman

We studied one metatarsus from the Turolian (MN12, 7.6–7.4/6.8 Ma [Hilgen et al., 2012]) locality of Kırşehir-Kaman (see Table 1). This fossil site, also known as Akkaşdağı, is located in the southern part of the Çankırı-Çorum Basin, 125 km southeast of Ankara (see Fig. 1) (Koufos and Vlachou, 2005). Mudstones, limestones, and sandstones with subordinate conglomerates and tuff compose the sedimentary succession and suggest an alluvial fan as the main depositional environment of the site (Kazanci et al., 2005). The main large mammals (e.g., carnivores, perissodactyls, artiodactyls, suids, and proboscideans) from this locality have been studied in detail by Antoine and Saraç (2005), de Bonis (2005), Kostopoulos and Saraç (2005), Koufos and Vlachou (2005), Liu and colleagues (2005), Saraç and Sen (2005), and Tassy (2005). More specifically in terms of equids, Koufos and Vlachou (2005) described the presence of four different *Hipparion* species: *Hipparion dietrichi*, *Hipparion moldavicum*, *Hipparion brachypus*, and *Hipparion* cf. *longipes*.

Muğla-Yatağan-Salihpaşalar 1

We studied one metatarsus from the Muğla-Yatağan-Salihpaşalar locality (see Table 1). This fossil site, which is found 5 km east of Salihpaşalar village (Muğla province) (see Fig. 1), was first described by Atalay (1980). The fossil-bearing red-bed unit belongs to the Yatağan Formation (Atalay, 1980; Geraads et al., 2002) and includes alternating conglomerates, sandstones, siltstones, and mudstones representing an alluvial flood plain depositional environment with braided stream channels (Kaya et al., 2012). The Turolian (MN12, 7.6–7.4/6.8 Ma [Hilgen et al., 2012]) ungulate mammalian faunal assemblage found at this fossiliferous locality is characterised by a high diversity of bovids and giraffes (Kaya et al., 2012), although it also includes several equid species such as *Hipparion mediterraneum* and *Hipparion matthewi* (Geraads et al., 2002; Saraç et al., 2002).

Muğla-Yatağan-Şerefköy

Two metatarsi from the Muğla-Yatağan-Şerefköy fossil site were analysed (see Table 1). This Turolian locality (MN12, 7.6–7.4/6.8 Ma [Hilgen et al., 2012]) is situated near the Şerefköy village, 9 km east of Yatağan town (Muğla province) (Kaya et al., 2012) (see Fig. 1). Muğla-Yatağan-Şerefköy also belongs to the Yatağan Formation (Kaya et al., 2012). Specifically, the fossil-bearing unit at this locality is composed of sandstones, siltstones, and mudstones and alternating fine- to coarse-grained conglomerates with subangular to subrounded gravel of pebble to cobble grade (Kaya et al., 2012). The depositional environment described is an alluvial flood plain with braided stream channels (Kaya et al., 2012). Hipparionines represent more than 50% of the entire faunal assemblage and can be grouped into five species belonging to three different morphotypes: *Cremohipparion* sp. type 1 (small-sized), *Cremohipparion* sp. type 2 (small-sized), "*Hipparion*" sp. type 1 (medium-sized), "*Hipparion*" sp. type 2 (medium-sized), and *Hippotherium brachypus* (large-sized) (Kaya et al., 2012).

Manisa-Düzpınar

We studied one metacarpus from the Manisa-Düzpınar fossil site (see Table 1), which is found in the outskirts of Develi village (Manisa province) (see Fig. 1). Fossil material was specifically collected from the light-coloured limestones, mudrocks, and sands that compose the water lacustrine deposits of the Urla Formation (Kaya et al., 1998). Micro- and macromammal fossil remains from this site have recently been reviewed by Mayda and colleagues (2015), who assigned the Develi fauna to the Miocene–Pliocene transition (MN13-14, 7.4/6.8–5.0 Ma [Hilgen et al., 2012]). Hipparionine material recovered at Manisa-Düzpınar was tentatively assigned to *Cremohipparion* cf. *matthewi* (Mayda et al., 2015).

Manisa-Aşağıçobanisa

We analysed one metatarsus from the Manisa-Aşağıçobanisa fossil site (see Table 1). This Plio-Pleistocene locality (MN15: 5.0–3.6/3.5 Ma, MN17: 2.5–2.0/1.8 Ma [Hilgen et al., 2012]) is situated in the vicinity of Aşağı Çobanisa village (Manisa province) (see Fig. 1), about 50 km northeast from Izmir (Mayda et al., 2013). Fossil remains were recovered from the fluvial deposits of the Turgutlu Formation, which mainly consists of cross-bedded sandstones and less commonly of interclasting mudrocks (Mayda et al., 2013). Equid material studied from this locality was assigned to *Equus* aff. *major*. It belongs to the mid-early Pleistocene (MN17, 2.5–2.0/1.8 Ma [Hilgen et al., 2012]) faunal association found at this locality, which is dated to 2.1–1.9 Ma (Mayda et al., 2013).

https://doi.org/10.1017/qua.2020.87 Published online by Cambridge University Press

Denizli-Pamukkale

One metacarpus from the middle Pleistocene (MN17-18, 2.5–0.6 Ma [Hilgen et al., 2012]) locality of Denizli-Pamukkale (see Fig. 1) was studied (see Table 1). Fossil remains at this site were recovered from the tourist travertine formations known as Pamukkale travertines (Rausch et al., 2019). These are freshwater limestones that form when hot ground water rich in calcium and bicarbonate emerges at springs (Guo and Riding, 1998). Specifically, fossils were collected from the 50-m-thick "Upper Travertine" unit (Lebatard et al., 2014), which represents travertine depositional environments (Rausch et al., 2019). This fossiliferous locality registers the presence of *E.* cf. *altidens* s.l. and *E.* cf. *apolloniensis* (Boulbes et al., 2014; Rausch et al., 2019).

Preparation and analysis of histological slides

Bone thin sections of ~100 µm thickness were prepared from each sample following standard procedures that include different steps of embedding, cutting, grinding, and polishing (Chinsamy and Raath, 1992). The obtained histological slides were observed and analysed under transmitted and polarized light to describe the bone histology and preservation. Specifically, we used a Nikon Eclipse E200 and a Zeiss Ax10 Lab.A1 polarising microscopes. High-quality micrographs were taken with the cameras (Canon EAOD 500D and Nikon DS-Fi1, respectively) attached to the different microscopes. Diagenetic alterations of the bone tissue were also studied in a desktop scanning electron microscope Phenom™ ProX.

Bone tissue types and their vascularization were qualitatively studied following classical approaches presented in the literature (e.g., Francillon-Vieillot et al., 1990; Chinsamy-Turan, 2005). Generally, bone tissue is classified as primary or secondary based on its origin. Primary bone is usually grouped into different typologies according to the degree of organization of the collagen fibres, the shape and arrangement of bone cells (i.e., osteocytes), and the quantity and organisation of the vascular canals (Francillon-Vieillot et al., 1990; Chinsamy-Turan, 2005; Huttenlocker et al., 2013). In large mammals, such as equids, during early ontogenetic stages primary bone is usually *fibrolamellar bone* tissue (Kolb et al., 2015b). This bone tissue is formed at high rates (Amprino, 1947; de Margerie et al., 2002), which results in a highly vascularized bone matrix with multiple primary osteons, many osteocytes, and randomly organized collagen fibres (Francillon-Vieillot et al., 1990; Chinsamy-Turan, 2005). When growth rate decreases as the animal approaches adult body size, *lamellar bone* tissue is deposited. In this case, it is usually called external fundamental system (EFS) or outer circumferential layer (OCL). Lamellar bone tissue is formed at slower rates than fibrolamellar bone (Amprino, 1947; de Margerie et al., 2002) and consists of highly organized collagen fibres, few vascular canals and/or primary osteons, and few osteocytes (Francillon-Vieillot et al., 1990; Chinsamy-Turan, 2005). Secondary bone, as the name suggests, is deposited after primary bone has been resorbed (Francillon-Vieillot et al., 1990; Currey, 2002). It results from the joint action of the osteoclasts (i.e., bone-resorbing cells) and the osteoblasts (i.e., bone-forming cells) during a process known as bone remodelling (Currey, 2002) or secondary reconstruction (Chinsamy-Turan, 2005). Secondary tissue may take the form of *secondary osteons* (also named Haversian canals) or can be endosteally formed, such as *compacted coarse cancellous bone* (Chinsamy-Turan, 2005).

Bone growth marks (BGMs, i.e., lines of arrested growth [LAGs] and annuli) (Castanet et al., 1993), both cyclical (CGMs) and non-cyclical ones (i.e., neonatal line [NL]) (Nacarino-Meneses and Köhler, 2018), were also analysed in the different cross sections. When possible, their perimeter was estimated using Image J software, and the results were plotted to reconstruct the pattern of metapodial growth (Nacarino-Meneses et al., 2016a). Size variation per year was calculated as a proxy of growth rate by subtracting BGMs' perimeters of consecutive annual growth cycles (Nacarino-Meneses et al., 2016a). The non-cyclical BGM described by Nacarino-Meneses and Köhler (2018) as the NL was considered as time zero for growth reconstructions (Woodward et al., 2013).

Several diagenetic features were recorded for each specimen, including the general histological index (GHI) (Hollund et al., 2012), the type of bone microscopic focal destruction (MFD) (Hackett, 1981), the presence and appearance of bone microcracks (Jans, 2005; Pfretzschner and Tütken, 2011), the degree of bone birefringence (Jans, 2005), and the presence of inclusions and infiltrations (Garland, 1989). The GHI (Hollund et al., 2012) was applied to qualitatively analyse the amount of unaltered microstructure within a bone cross section. Based on previous preservation indexes that only considered microorganisms as the main factors altering bone tissue microstructure (Hedges et al., 1995; Millard, 2001; Haynes et al., 2002), the GHI assesses the amount of bone microstructure affected by bioerosion, microcracks, and infiltrations (Hollund et al., 2012). According to this preservation index (Hollund et al., 2012), we classified the microscopic damage into each of the already described six categories that range from GHI 0 (bad preservation) to GHI 5 (excellent preservation). We also examined the presence and type of MFD within each bone slide. These features, also known as tunnels or foci, are changes of the bone tissue caused by the action of microorganisms (Hackett, 1981). MFD is classified into four types on the basis of their size, shape, and the presence of a hypermineralized ring (Hackett, 1981; Jans, 2008); the four types are Wedl, linear longitudinal, budded, and lamellate. To simplify our results, linear longitudinal, budded, and lamellate foci where all classified as non-Wedl tunnels following Jans (2008). Furthermore, we preferentially used the term "Wedl-like" instead of "Wedl" because the agent causing this kind of borings in our sample is probably different from that causing the tunnels originally described by Wedl (i.e., cyanobacteria, Turner-Walker, 2019). Bone microcracks or microfissures, on the other hand, tend to appear in bone cross sections as a result of

https://doi.org/10.1017/qua.2020.87 Published online by Cambridge University Press

variations in the water content (i.e., wetting and drying cycles that provoke shrinkage and expansion) of the bone matrix collagen during early stages of fossilization (Pfretzschner, 2000, 2004; Pfretzschner and Tütken, 2011). Here, we qualitatively describe the presence and extent of bone microcracks for each fossil sample. Bone birefringence is related to the degree of arrangement of the apatite crystals, with ordered apatite crystals showing a high degree of birefringence (Schoeninger et al., 1989). In the present work, bone birefringence was assessed as 1 (perfect), 0.5 (reduced), or 0 (absent) following Jans (2005). Finally, we analysed inclusions and infiltrations within each bone cross section. According to Garland (1989), inclusions appear within bone spaces (e.g., medullary cavity, Haversian canals) while infiltrations appear within the bone substance itself. Inclusions can consist of diverse materials such as sand, minerals, or microorganisms (Jans et al., 2002). Infiltrations, on the other hand, appear as stains in the bone section (Jans et al., 2002).

RESULTS

Bone histology and skeletochronology

Primary bone tissue of Turkish hipparionines is characterized by the presence of longitudinal primary osteons (POs) oriented in circumferential rows (see Fig. 2A) throughout the whole bone cortex. In KK-1 we additionally identified compacted coarse cancellous bone (CCCB) composing most of the inner bone cortex (see Fig. 2B). Abundant secondary osteons (SOs) are scattered in the cortex of Turkish *Hipparion* (see Fig. 2B), which eventually form a well-developed Haversian bone (see Fig. 2C) in some specimens like UEK-1. Secondarily deposited endosteal bone (EB) lines the medullary cavity of several hipparionine samples (e.g., UEK-1, MD-7, CG-1) (see Fig. 2D).

Bone tissue types of our *Equus* sample was only studied in the Denizli-Pamukkale metacarpus (P-1, see Fig. 2E, 2F) since the histology of the other *Equus* sample was not well preserved (see below). The internal cortex of this specimen consists of a fibrolamellar bone tissue with circumferentially oriented vascular canals (PO), which conforms to the primary bone tissue type known as laminar bone (LB) (see Fig. 2E). Vascular canals within the external half of the cortex predominantly have a longitudinal orientation (see Fig. 2E), resulting in longitudinal POs oriented in circumferential rows (see Fig. 2E). Scattered SOs are also identified in this *Equus* specimen (see Fig. 2F), mainly in the posterior part of the cortex. EB is found in the innermost cortex.

BGMs, both in the form of LAGs and annuli, were also identified in *Hipparion* and *Equus* samples (see Fig. 3). These features were recognized in many of the specimens under analysis (CG-1, CG-2, CG-3, P-1, MD-7, MYSA-1, UEK-1), regardless of the preservation state (see Fig. 3A) or the degree of intracortical remodelling (i.e., presence of multiple SOs) (see Fig. 3B). However, the complete path of the BGMs within the whole cortex could only be followed with confidence in the metacarpus MD7 (see Fig. 3C), which presents one NL and six CGMs (see Fig. 3C). All BGMs in this specimen appear within the fibrolamellar bone tissue, and no EFS/OCL was recognized. The perimeter of each CGM, as well as that of the NL, was measured and plotted to reconstruct the pattern of MD7's growth (see Fig. 3D). As Figure 3D shows, this bone grows faster during the first year of life and then progressively reduces its growth rate. Minimal rates of bone deposition are only attained after the deposition of the fourth CGM (see Fig. 3E). This change in growth rate observed in both graphs (see Fig. 3D, 3E) coincides with a decrease in the spacing between CGMs (see Fig. 3C).

Preservation at the histological level

Bone preservation at the histological level varies greatly among the samples studied (see Fig. 4A, 5). Only two of the specimens under analysis (Supplementary Table 1), which represent 14.3% of the sample (see Fig. 4A), present diagenetically unaltered histology (GHI = 5, see Fig. 5A). Bone histological features can also be easily identified in P-1 (see Fig. 5B), which is categorized as GHI = 4 (see Fig. 4A, Supplementary Table 1) due to the high number of bone microcracks that run through its cortex (see Fig. 5B). Bone microstructure is completely altered in four metapodia (28.6% of the sample, see Fig. 4A, Supplementary Table 1), which are scored as GHI = 0 (see Fig. 5E). The remaining specimens under analysis also present altered histological preservation: five (35.7% of the sample, see Fig. 4A, Supplementary Table 1) are classified as GHI = 1 (see Fig. 5D) and two (14.3% of the sample, see Fig. 4A, Supplementary Table 1) as GHI = 2 (see Fig. 5C) according to the amount of bone microstructure preserved in the different cross sections (Hollund et al., 2012). Specimens found within fluvial and alluvial sediments usually present worse histological preservation (lower GHI) than those recovered from lacustrine and travertine environments (Table 2), though some exceptions can be found. UEK-1, for example, was recovered from an alluvial fan (see Table 2) but presents very well-preserved histology (see Fig. 5A, Supplementary Table 1). Thus, there is not a clear trend in the relationship between the degree of bone preservation and its depositional environment.

MFD (see Fig. 6) is extensive (see Supplementary Table 1), affecting 78.6% of the sample (see Fig. 4B). In very badly preserved specimens (GHI = 0), MFD is widely distributed across the whole cortex (see Fig. 5E), while it is restricted to the internal and/or the external cortex in those samples categorized as GHI = 1 and GHI = 2 (see Fig. 5C, 5D). Non-Wedl tunnels (see Fig. 6A–I) are recognized in 71.4% of the sample (see Fig. 4B, Supplementary Table 1), both in the form of budded (~50 µm diameter, see Fig. 6A–C) and linear longitudinal (~20 µm diameter, see Fig. 6D–F) tunnels. In transmitted light microscopy, both foci present a rim that isolates them from the surrounding alterations (see Fig. 6A, 6D). This rim is not always recognizable, however, when samples are observed under scanning electron microscopy (SEM) (see Fig. 6B, 6C, 6E, 6F). Nonetheless, SEM always allows the identification of the submicron porosity (see Fig. 6C, 6F) characteristic of non-Wedl MFD (Turner-Walker et al., 2002).

https://doi.org/10.1017/qua.2020.87 Published online by Cambridge University Press

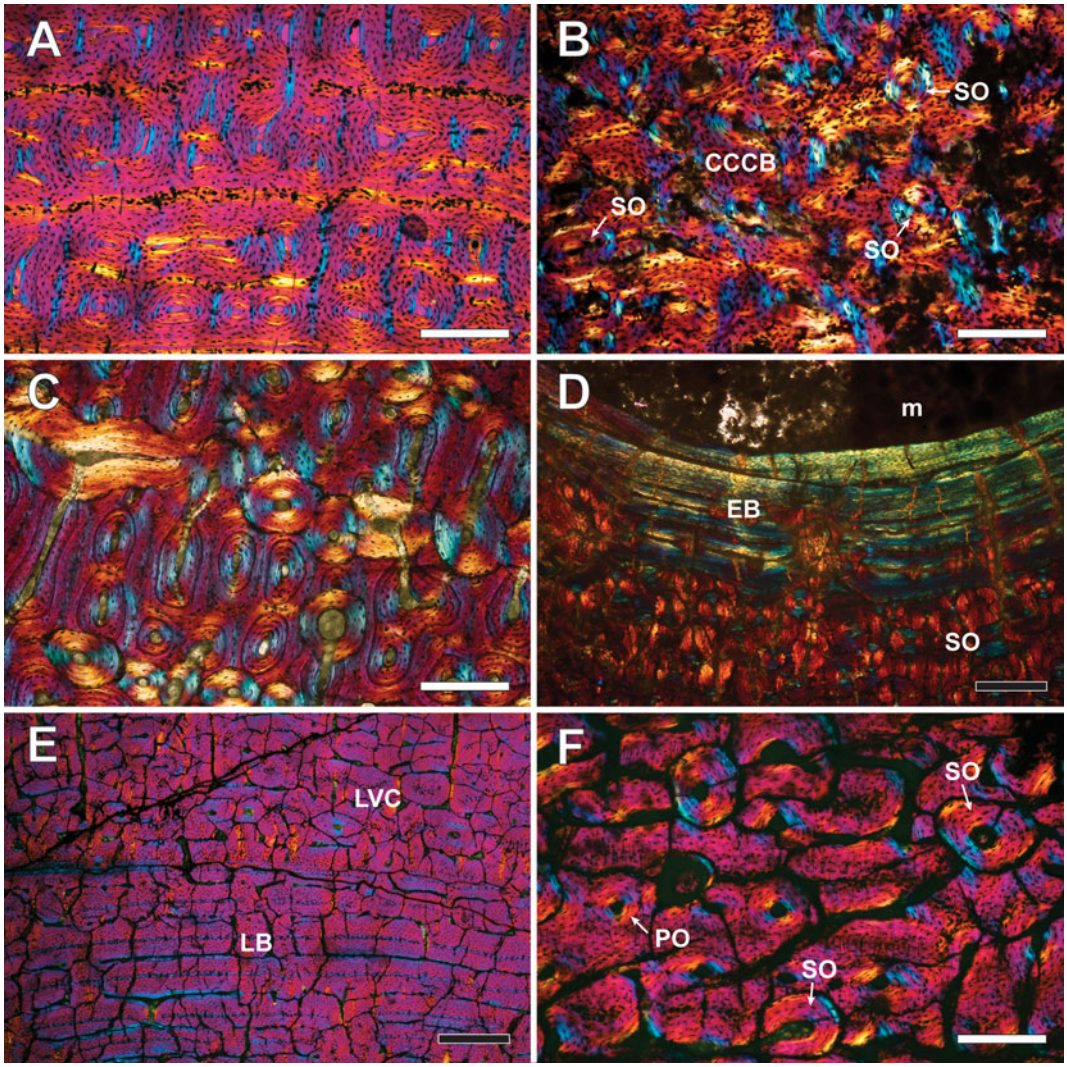

Figure 2. (color online) Bone tissue types in metapodial cortices of extinct equids from Turkey. (A) *Hipparion*, specimen MD-7. POs oriented in circumferential rows. (B) *Hipparion*, specimen KK-1. Compacted coarse cancellous bone (CCCB) with scattered secondary osteons (SOs). (C) *Hipparion*, specimen UEK-1. Well-developed Haversian bone with multiple SOs. (D) *Hipparion*, specimen UEK-1. Endosteal bone (EB) and SOs; m = medullary cavity. (E) *Equus*, specimen P-1. Vascular canals present a circumferential orientation (laminar bone, LB) in the most internal half of the cortex but are oriented longitudinally (LVC) in the external half of the cortex. (F) *Equus*, specimen P-1. Scattered SO found in P-1. Images show bone cross sections observed under polarized light with 1/4λ plate. White scale bars: 250 µm; black scale bars: 500 µm.

The generalized damage of the bone tissue in several specimens, such as MYSE-2, greatly hampers the identification of the different types of MFD (Wedl-like vs. non-Wedl tunnels) when analysed under transmitted light (see Fig. 6G). Such specimens examined under SEM show an almost complete destruction of the bone microstructure (see Fig. 6H, 6I) that likely result from the dissolution and re-precipitation of the bone matrix (Turner-Walker, 2012). With SEM, we also identified non-Wedl submicron porosity (see Fig. 6I). Wedl-like tunnels (see Fig. 6J–L), on the other hand, are only found in one sample: KK-1 (see Fig 4B, Supplementary Table 1). In this specimen, branching Wedl-like tunnels seem to start from the lumen of the vascular canal and progress outwards within the cortical bone (see Fig. 6J–L). Interestingly, Wedl-like MFD appears both in the most external cortex and in the middle area of the compacta. When observed under SEM, bone matrix of KK-1 also shows signs of dissolution and precipitation, as well as multiple breakages in disaggregated fragments (see Fig. 6K–L).

Bone microcracks are only found in two metapodials (14.3% of the sample, see Fig. 4C): P-1 and UEK-1 (see Fig. 7, Supplementary Table 1). In P-1, microfissures extend through the whole cortical bone, from the periosteal to the endosteal surface (see Fig. 5B). Interestingly, they interrupt the primary bone tissue without following any preferential direction. As a result, both radial and circumferential cracks can be detected within the fibrolamellar bone (see Fig. 5B). On the contrary, microcracks within SOs follow the path of the cement line and never trespass it (see Fig. 7A). In UEK-1, bone microcracks are limited to a few SOs (see Fig. 7B). In this case, microfissures appear radial to the Haversian canal crossing the cement line (see Fig. 7B).

https://doi.org/10.1017/qua.2020.87 Published online by Cambridge University Press

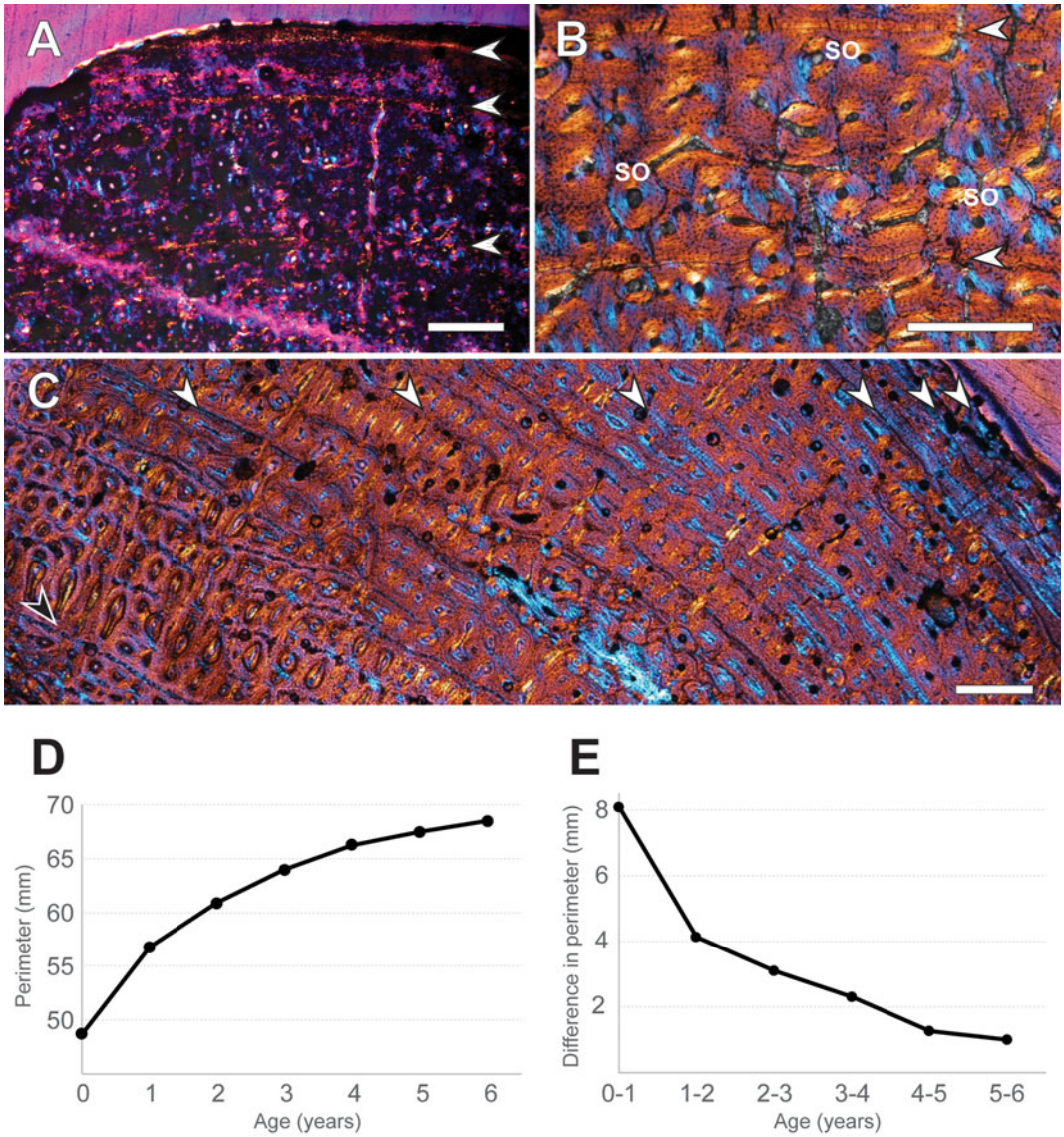

Figure 3. (color online) Bone growth marks (BGMs) in metapodial cortices of extinct equids from Turkey. (A) *Hipparion*, specimen CG-1. BGMs can still be recognized despite poor histology preservation. (B) *Hipparion*, specimen UEK-1. BGMs are still identifiable despite a high concentration of secondary osteons (SO). (C) *Hipparion*, MD-7. Non-cyclical (neonatal line [NL], black arrowhead) and cyclical growth marks (CGMs, white arrowheads) are identified. (D) Growth curve obtained for MD-7 by plotting the perimeter of each BGM (mm, ordinate axis) against the estimated age (years, abscissa axis). (E) Difference in perimeter of consecutive BGM (mm, ordinate axis) is plotted against estimated age (years, abscissa axis) in MD-7, providing a proxy of the growth rate of the bone. Images show bone cross sections observed under polarized light with 1/4λ plate. Scale bars: 500 µm.

The medullary cavity of almost all specimens under study, as well as most of the pore spaces and resorption cavities of their cortices, are infilled with mineral sediments (see Supplementary Table 1). These are either a muddy clastic material (see Fig. 2D) or crystals of quartz, depending on the geology of the area. A red-brown staining, which likely results from the infiltration of humic factors (Jans et al., 2002), is also locally found in most of the bone cortices under analysis (see Fig. 5B, 5D, Supplementary Table 1).

Birefringence is preserved in 85.8% of the sample (see Fig. 4D), but substantially reduced in 6 out of the 12 specimens that still present this histological feature (see Fig. 4D, Supplementary Table 1), indicating a disruption of the collagen-hydroxyapatite bond in these fossil samples (Turner-Walker, 2008).

DISCUSSION

Bone histology and life history of Turkish fossil equids

The histology of fossil bone and, in particular, features such as the type of bone tissue, the pattern of vascularization, and the presence of growth marks are useful when undertaking life history studies of extinct taxa (e.g., Chinsamy-Turan,

https://doi.org/10.1017/qua.2020.87 Published online by Cambridge University Press

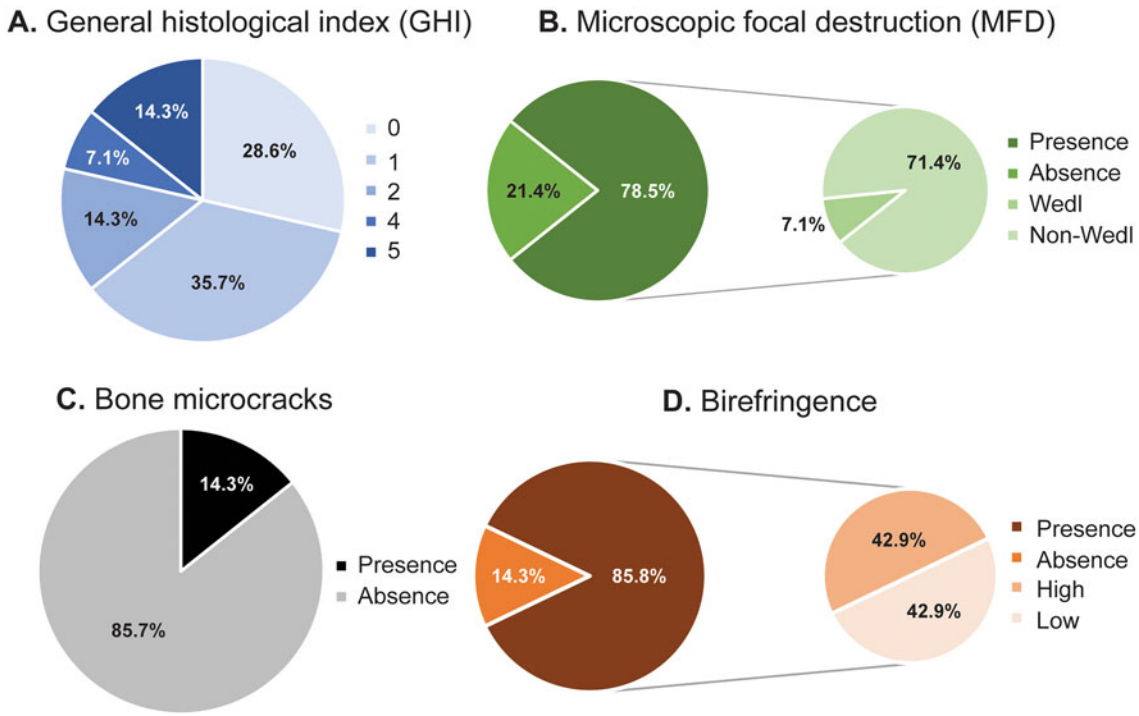

Figure 4. (color online) Pie charts showing the prevalence of different diagenetic features in the metapodia of extinct equids from Turkey. Percentage values for each group are shown.

2005, 2012). The cortices of the metapodia of the Turkish fossil equids consist of a fibrolamellar complex with longitudinal POs oriented in circumferential rows (see Fig. 2A). These histological characteristics have been previously reported in several *Hipparion* (Martínez-Maza et al., 2014; Orlandi-Oliveras et al., 2018) and *Equus* (Nacarino-Meneses et al., 2016a; Nacarino-Meneses and Orlandi-Oliveras, 2019) species. The presence of CCCB in the *Hipparion* metatarsus

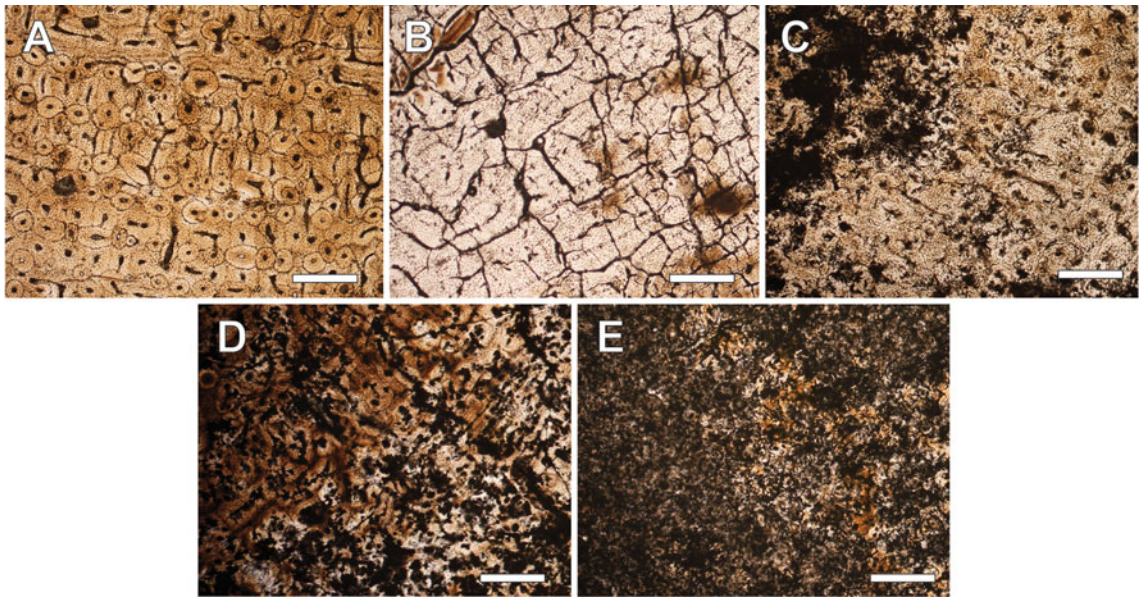

Figure 5. (color online) Preservation states (general histological index [GHI]) identified in the metapodia of extinct equids from Turkey. (A) *Hipparion*, specimen UEK-1. Well-preserved histology, directly comparable to histology of modern bone (GHI = 5). (B) *Equus*, specimen P-1. Bone tissue is fairly well preserved, although lots of microcracks run through the cortex (GHI = 4). (C) *Hipparion*, specimen KK-1. Some well-preserved bone microstructure is recognised between altered areas (GHI = 2). (D) *Hipparion*, specimen MYSA-1. Only small areas of well-preserved bone tissue are present (GHI = 1). (E) *Hipparion*, specimen MYSE-2. Histology is completely altered with no original histological features identifiable (GHI = 0). Images show bone cross sections observed under transmitted light. Scale bars: 500 µm.

https://doi.org/10.1017/qua.2020.87 Published online by Cambridge University Press

Table 2. Summary of the main preservation results and the depositional environment for the different fossil sites studied. Data on depositional environment from (a) Forsten and Kaya (1995), (b) Kaya (1981), (c) Kaya and colleagues (2005b), (d) Seyitoğlu and colleagues (2009), (e) Tekkaya and colleagues (1975), (f) Kazanci and colleagues (2005), (g) Kaya and colleagues (2012), (h) Kaya and colleagues (1998), (i) Mayda and colleagues (2013), (j) Rausch and colleagues (2019).

Epoch (MN)	Locality	General histological index (GHI)	Kind of MFD	Presence of microcracks	Birefringence	Depositional environment
Late Miocene (MN11-12)	Çanakkale-Gülpınar	1	Non-Wedl	No	Low	Fluvial[a]
	Izmir-Karaburun	1	Non-Wedl	No	High	Fluvial[b]
	Kütahya-Bayat	1	Non-Wedl	No	High	Alluvial channel[c]
	Uşak-Kemiklitepe 2	5	-	Yes	High	Alluvial fan[d]
	Çankırı-Yeniköy	0	Non-Wedl	No	Low	Alluvial flood plain[e]
Late Miocene (MN12)	Kırşehir-Kaman	2	Wedl	No	High	Alluvial fan[f]
	Muğla-Yatağan-Salihpaşalar 1	2	Non-Wedl	No	Low	Alluvial flood plain[g]
	Muğla-Yatağan-Şerefköy	0	Non-Wedl	No	Low	Alluvial flood plain[g]
Miocene–Pliocene (MN13-14)	Manisa-Düzpınar	5	-	No	High	Lacustrine[h]
Early Pleistocene (MN17)	Manisa-Aşağıçobanisa	1	Non-Wedl	No	Low	Fluvial[i]
Early Pleistocene (MN17-18)	Denizli-Pamukkale	4	-	Yes	High	Travertine[j]

KK-1 is noteworthy since such tissue has not previously been reported in fossil horses (see Fig. 2B). This endosteally formed bone tissue results from the incorporation and compaction of metaphyseal bone trabeculae into the diaphyseal cortex during longitudinal growth (Enlow, 1962; Chinsamy-Turan, 2005). Although it may appear in the mid-diaphysis of long bones (McFarlin et al., 2008; Geiger et al., 2013; Kolb et al., 2015b; Montoya-Sanhueza and Chinsamy, 2017; Legendre and Botha-Brink, 2018; Bhat et al., 2019; Garrone et al., 2019), CCCB is most commonly found in metaphyseal areas (Enlow, 1962). KK-1 was prepared from the most distal part of the bone shaft (see Supplementary Fig. 1), which explains the presence of this bone tissue type in the cross section.

Another interesting finding was the distinctive stratification present in the proximal section of an *Equus* metacarpus, P-1 (see Supplementary Fig. 1): multiple circumferentially oriented vascular canals (i.e., LB) occur in the inner half of the cortex while longitudinal POs were present in the outer half of the cross section (see Fig. 2E). Patches of LB have previously been identified in the inner metapodial cortex of hipparionines from Greece and Spain (Orlandi-Oliveras et al., 2018), as well as in that of *Equus hemionus* (Nacarino-Meneses et al., 2016a), but never as extensively developed as in our specimen P-1. The abrupt change in the orientation of the vascular canals in *Equus hemionus* appears to be linked to birth (Nacarino-Meneses et al., 2016b), although in the latter instance the vascular canals change from a longitudinal to a circumferential orientation (Nacarino-Meneses et al., 2016b). We propose that the change in vascular channel orientation observed in P-1 (see Fig. 2E) may also be related to the birth of the animal, as it likely reflects the changes in biomechanics and growth rate associated with the beginning of postnatal life (Nacarino-Meneses and Köhler, 2018).

Life history studies on extinct taxa usually involve the analysis of BGMs, as they provide key information about traits such as the age at death, the age at maturity, or the growth rate (Woodward et al., 2013; Nacarino-Meneses et al., 2016a). Unfortunately, the diagenetic alteration of most of our samples greatly hampered the identification of these histological features (see Fig. 3A). Nevertheless, among all our material, BGMs were well preserved in MD-7 (see Fig. 3C), a metacarpal recovered from the Mio-Pliocene fossil locality of Manisa-Düzpınar, which is considered to belong to the medium-sized equid *Cremohipparion* cf. *matthewi*—the only equid known from this locality (Mayda et al., 2015). In this specimen, five CGMs plus one NL were observed in the cross section, and an EFS/OCL was not identified in the most external cortex (see Fig. 3C). This finding agrees with descriptions for the Pleistocene species *Equus steinheimensis* (Nacarino-Meneses and Orlandi-Oliveras, 2019), but differs from previous findings in Spanish and Greek hipparionines, in which an EFS/OCL usually appears after the second or third year of growth (i.e., second or third CGM) (Martínez-Maza et al., 2014; Orlandi-Oliveras et al., 2018). The presence of an EFS/OCL in metapodial cross sections of equids indicates the end/decrease of periosteal bone growth (Nacarino-Meneses et al., 2016a). Hence, the lack of EFS/OCL in *Cremohipparion* cf. *matthewi* specimen MD-7 suggests an extended period of periosteal growth (Nacarino-Meneses et al., 2016a) as compared to other European hipparionines. In these taxa, the EFS/OCL has been correlated with the attainment of skeletal maturity (Martínez-Maza et al., 2014; Orlandi-Oliveras et al., 2018); therefore, the absence of the EFS/OCL (despite having at least 5–6 years of growth) in *Cremohipparion* cf. *matthewi* may indicate extended skeletal maturity. In equids, skeletal

https://doi.org/10.1017/qua.2020.87 Published online by Cambridge University Press

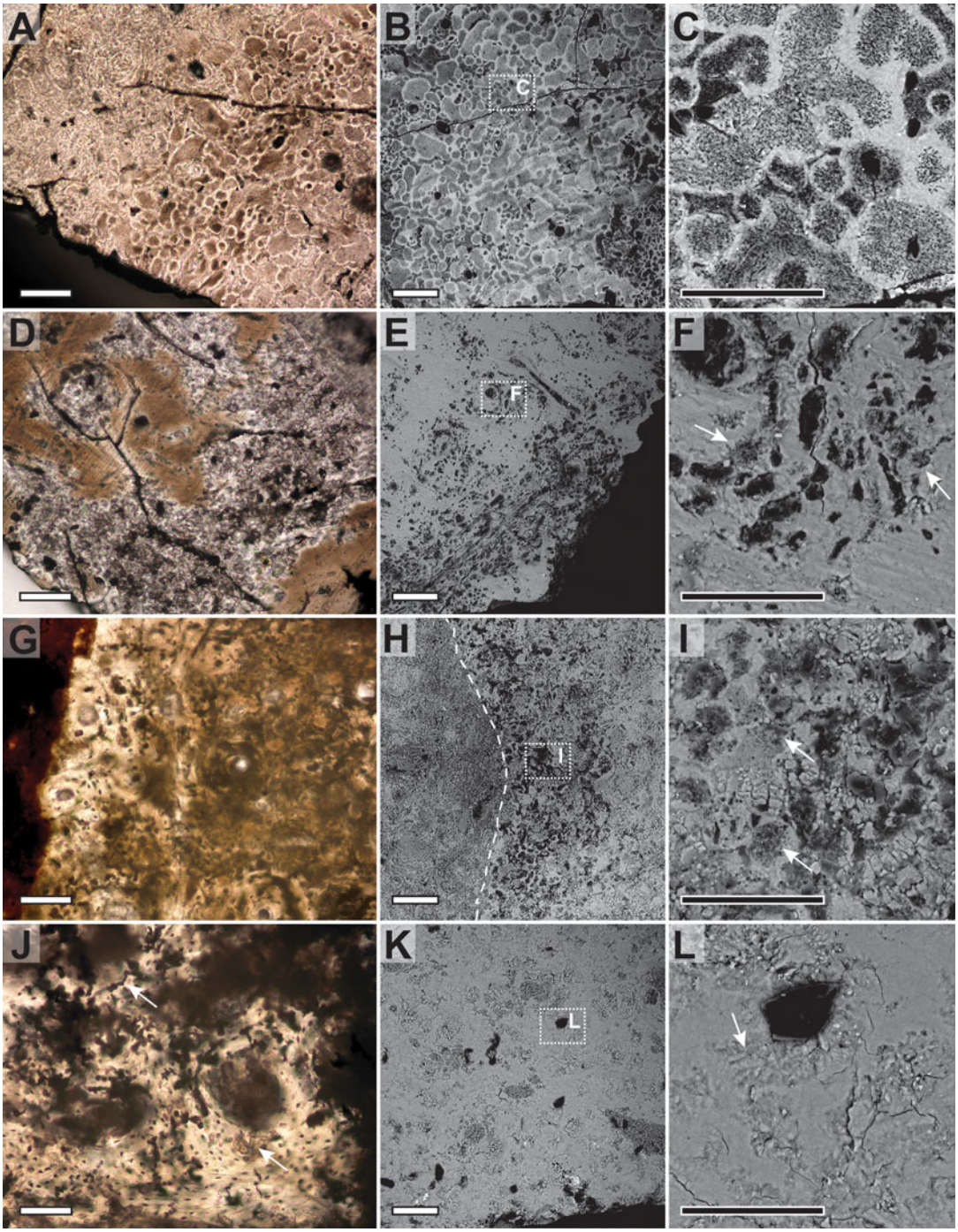

Figure 6. (color online) Microscopic focal destruction (MFD) in the metapodia of extinct equids from Turkey. (A) *Hipparion*, specimen CG-2. Transmitted light micrograph showing multiple non-Wedl tunnels of ~50 μm diameter. (B) *Hipparion*, specimen CG-2. SEM micrograph of the same area showing bacterial damage. (C) *Hipparion*, specimen CG-2. Detailed SEM micrograph showing submicron porosity surrounded by a hypermineralized ring around each bacterial colony. (D) *Hipparion*, specimen KB-1. Transmitted light micrograph showing non-Wedl tunnels of ~20 μm diameter. (E) *Hipparion*, specimen KB-1. SEM micrograph of the same area showing bacterial damage. (F) *Hipparion*, specimen KB-1. Detailed SEM micrograph showing the submicron porosity characteristic of bacterial damage. Note that no hypermineralized ring surrounds submicron pores (arrows) in this case. (G) *Hipparion*, specimen MYSE-2. Transmitted light micrograph showing extensive damage through the cortex. It is difficult to recognize either Wedl-like or non-Wedl tunnels because the overall bone microstructure is destroyed. (H) *Hipparion*, specimen MYSE-2. SEM micrograph of the same area showing general destruction of the bone microstructure. Bone matrix (right of dashed line) is almost indistinguishable from mineral inclusions (left of dashed lines). (I) *Hipparion*, specimen MYSE-2. Detailed SEM micrograph showing submicron porosity (arrows) characteristic of bacterial damage. (J) *Hipparion*, specimen KK-1. Transmitted light micrograph showing Wedl-like tunnels (arrows). (K) *Hipparion*, specimen KK-1. SEM micrograph of the same area showing microscopic damage. (L) *Hipparion*, specimen KK-1. Detailed SEM micrograph showing Wedl-like tunnels (arrows) that may have been caused by algae. White dotted rectangles in B, E, H, and K indicate areas of image magnification showed in C, F, I, and L, respectively. White scale bars: 100 μm, black scale bars: 50 μm.

https://doi.org/10.1017/qua.2020.87 Published online by Cambridge University Press

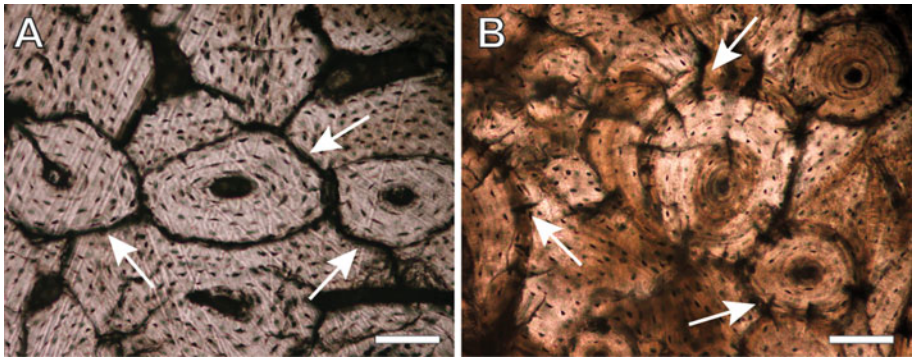

Figure 7. (color online) Bone microcracks in the secondary bone tissue of extinct equids from Turkey. (A) Circumferential cracks (arrows) following the cement line of SOs in P-1. (B) Radial fissures (arrows) in the cement lines of SOs in UEK-1. Images show bone cross sections observed under transmitted light. Scale bars: 100 µm.

maturity of the bone (understood as the time of epiphyseal fusion or the end of longitudinal bone growth) can also be inferred from growth curve reconstructions (Nacarino-Meneses et al., 2016a). In the histological study of *Equus hemionus*, Nacarino-Meneses and colleagues (2016a) demonstrated that the completion of longitudinal bone growth correlates with a decrease in periosteal growth and that growth rate is minimal after epiphyseal fusion. Although metacarpal MD-7 of *Cremohipparion* cf. *matthewi* shows a decrease in growth rate after the deposition of the first CGM (see Fig. 3D), growth rate continues at a similar rate until the fourth CGM (fifth year of life), after which it becomes minimal (see Fig. 3E). This suggests that epiphyses of MD-7 would have fused after the fourth year of life, much later than in similar body-sized Spanish and Greek *Hipparion* horses (Martínez-Maza et al., 2014; Orlandi-Oliveras et al., 2018), and also points to a delayed skeletal maturity for the species. These inferences, however, should be considered with caution due to our limited sample size, as they only provide preliminary life history information for this hipparionine that must be tested in future studies.

Histotaphonomy of Turkish fossil equids

Bone degradation is abundant in our sample, affecting almost 80% of the bones studied (see Fig. 4B). Non-Wedl tunnels (see Fig. 6A–I) are the main MFD identified both in *Hipparion* and *Equus* specimens (see Fig. 4B, Supplementary Table 1), while Wedl-like tunnelling only affects the hipparionine metatarsal KK-1 (see Fig. 4B, 6J–L, Supplementary Table 1). This contrasts with previous research in fossils reporting a higher or even an exclusive presence of Wedl tunnels (Trueman and Martill, 2002; Bao et al., 2009; Chinsamy-Turan and Ray, 2012), but agrees with the research of Mayer and colleagues (2020) and Turner-Walker (2012), who describe non-Wedl microboring as the primary MFD affecting mammalian bones recovered from the palaeontological fossil record. It should be considered that non-Wedl tunnels are much easier to identify than Wedl ones in poorly preserved samples (Mayer et al., 2020), so the huge alteration of most of our specimens (see Fig. 4A, 5D–E) might be partially biasing our findings toward the identification of non-Wedl tunnels, as proposed in other investigations (Mayer et al., 2020).

Wedl and non-Wedl tunnels are traditionally believed to register the action of different microorganisms (Jans, 2008). Since Hackett (1981), non-Wedl MFD is usually attributed to bacteria (Jans, 2008), while Wedl foci are thought to be caused by fungi (Marchiafava et al., 1974), algae (Davis, 1997; Fernández-Jalvo et al., 2010), and/or cyanobacteria (Davis, 1997; Turner-Walker and Jans, 2008). Recently, several authors have argued that both kinds of MFD are just the result of specific bacteria boring different tissue types and that tunnelling type cannot be assigned to different decomposition agents (Kendall et al., 2018; Turner-Walker, 2019). Here, we follow the classical approach that correlates the MFD observed in our sample with different microbes (e.g., Jans, 2008). Thus, the identification of Wedl-like tunnels on the *Hipparion* specimen KK-1 (see Fig. 4B, Fig. 6J–L, Supplementary Table 1) suggests that it was affected by microorganisms other than bacteria (Jans, 2008). This kind of MFD has traditionally been associated with fungi (Marchiafava et al., 1974; Hackett, 1981; Trueman and Martill, 2002; Jans et al., 2004; Chinsamy-Turan and Ray, 2012), but, as already stated, it is known that other microbes like cyanobacteria or algae can also leave Wedl-like borings in the bone tissue (Turner-Walker and Jans, 2008; Fernández-Jalvo et al., 2010; Turner-Walker, 2019). It has been proposed that the depositional environment of the specimen might be key to establishing the main agent of the Wedl tunnelling, as fungi will only be expected in terrestrial environments, while cyanobacteria and algae occur in aquatic environments (Kendall et al., 2018). Metacarpal KK-1 was recovered from an alluvial fan (Kazanci et al., 2005), so aquatic microorganisms cannot be excluded as bioerosion agents. Indeed, the morphology and the specific location of the Wedl-like tunnelling around vascular canals (see Fig. 6J–L) throughout the entire middle and external cortex of KK-1 agrees with previous descriptions of borings caused by algae (Fernández-Jalvo et al., 2010; Fernández-Jalvo and Andrews, 2016). These microorganisms, along with moss and lichen, are known to penetrate the bone through its histological traits (Fernández-Jalvo et al.,

https://doi.org/10.1017/qua.2020.87 Published online by Cambridge University Press

2010), while fungal and cyanobacterial damage usually starts at the periosteal surface and is commonly restricted to the most external part of the bone cortex (Jans, 2008; Bao et al., 2009). Previous taphonomic research performed at this specific fossil site report macroscopic alterations by roots, fungi, and other microorganisms (Valli, 2005), so we also cannot completely discard fungal damage to KK-1. However, the location of the MFD in the section likely points toward freshwater algae (which may be included in "other microorganisms" [Valli, 2005]) as the main agent causing the microboring in this sample.

The high presence of non-Wedl tunnels in the fossil *Hipparion* and *Equus* metapodia (see Fig. 4B, Fig. 6A–I, Supplementary Table 1), on the other hand, suggests bacterial degradation (Jans, 2008). Corpse-decomposing bacteria consists both of exogenous bacteria from the soil (Turner-Walker, 2008; Kontopoulos et al., 2016; Morales et al., 2018; Galligani et al., 2019) and of intrinsic gut microbiota, including bacteria (Child, 1995; Bell et al., 1996; Jans et al., 2004; Hollund et al., 2012; White and Booth, 2014; Damann and Jans, 2017; Brönnimann et al., 2018). Currently there is no consensus as to which kind of bacteria has a greater influence on bone bioerosion. Following the "endogenous model," Jans and colleagues (2004) proposed that animal remains from archaeological sites may present low bacterial damage because specimens are usually buried as fragments without flesh (i.e., butchered animals), preventing putrefaction bacteria from spreading from the belly to the limbs (Jans et al., 2004). The larger prevalence of bacterial attack in our samples (see Fig. 4B, Fig. 6A–I, Supplementary Table 1) may suggest that the *Hipparion* and *Equus* fossil specimens analysed here would have entered the fossil record as complete animals, facilitating the invasion of endogenous bacteria throughout the body (Jans et al., 2004). This hypothesis, however, seems highly improbable, as fossil bones usually enter the soil as fragments because of the previous action of scavengers (Trueman and Martill, 2002). Indeed, recent studies propose that exogenous bacteria may contribute more to bioerosion (Turner-Walker, 2008; Kendall et al., 2018) than intrinsic gut microbiota because most decomposing bacteria is already present in the soil (Metcalf et al., 2016). This has been claimed to be particularly true for tropical and subtropical climates (Morales et al., 2018; Galligani et al., 2019). Palaeoenvironmental reconstructions for Turkey suggest a dry, warm-temperate climate from the Miocene (Akgün et al., 2007; Akkiraz et al., 2011; Kayseri-Özer et al., 2017) to the early Pleistocene (Kahlke et al., 2011; Jiménez-Moreno et al., 2015), with warmer temperatures than today (Jiménez-Moreno et al., 2015). This palaeoclimatic scenario could have led to higher soil bacterial decomposing activity (Galligani et al., 2019) that might have been responsible for the large prevalence of bacterial attack observed in fossil *Hipparion* and *Equus* samples (see Fig. 4B, Fig. 6A–I, Supplementary Table 1).

In addition to temperature, other physical aspects of the environment, such as oxygen and water, also play a key role in the preservation of the bone microstructure, as they control the action of the different microorganisms (Kendall et al., 2018). Bones buried in waterlogged and anoxic conditions, for example, are not usually affected by microbial attack, while soils with periodical or seasonal influx of water and variation in temperature favour microboring (Hackett, 1981). We propose that the greatly degraded samples analysed here (GHI = 0–2, see Fig. 5D, 5E, Supplementary Table 1) may have experienced variation in moisture during early stages of diagenesis. Interestingly, some of the most altered specimens of our sample belong to alluvial flood plain depositional environments (e.g., CY-1, MYSE-1, see Table 2, Supplementary Table 1), which are prone to periodic inundations. These wetting-drying, low-high oxygen cycles may have influenced the quick degradation of the bones. Specimens UEK-1, MD-7, and P-1, on the other hand, were not affected by any kind of MFD (GHI = 4–5, see Fig. 5A, 5B, Supplementary Table 1), so we propose that they were probably buried in anoxic waterlogged soils. Indeed, in UEK-1 the occurrence of radial microcracks that cross the cement lines of SOs (see Fig. 7B) also suggest that fossilization occurred in an aquatic environment (Pfretzschner, 2004; Pfretzschner and Tütken, 2011; Tomassini et al., 2015). According to Pfretzschner (2004), these radial microfissures appear in response to the swelling of bone collagen by water during the late stage of early diagenesis, which creates a tension stress in the cement line that triggers breakage. Variations in the water content of the collagen may also be responsible for the microscopic breakages of the bone matrix observed in SEM (see Fig. 6H, 6I, 6K, 6L). Bone microcracks were also identified in P-1 (see Supplementary Table 1), both within the fibrolamellar bone (see Fig. 5B) and within areas of secondary bone tissue (see Fig. 7A). However, unlike in UEK-1 (see Fig. 7B), bone microcracks in the areas of SOs in P-1 follow the cement lines and never cross them (see Fig. 7A).

Interestingly, P-1 was recovered from an exceptional depositional environment: the Pamukkale travertines (Rausch et al., 2019). These are sedimentary rocks formed by the precipitation of carbonates in geothermally heated hot-springs (Guo and Riding, 1998). Since intense heat is known to provoke fractures in the bone tissue (Hanson and Cain, 2007), the microcracks observed in P-1 may be the result of its fossilization in a hot environment. When temperatures exceed 100°C the heat can cause the denaturation of collagen in mineralized bones (Bonar and Glimcher, 1970) as a result of the breakage of the triple-helical chains, the disruption of intermolecular cross-links, and the shrinkage of the collagen molecules (Lees, 1989). Maximum palaeotemperatures inferred for the Quaternary deposits of the Pamukkale travertines are only 70°C (Özkul et al., 2013), so bone collagen would have not completely denatured in this environment. It may have suffered, however, some structural changes that may have led to bone microcracks, including the unravelling of the helical chains, which may occur at lower temperatures (Lees, 1989). Indeed, heating affects the collagen fibrils differently as compared to variations in water content: while water absorption/adsorption causes changes at right angles (radially) to the collagen fibril direction (Pfretzschner, 2004), thermal shrinkage provokes the longitudinal breakage of the collagen fibrils

https://doi.org/10.1017/qua.2020.87 Published online by Cambridge University Press

(Bonar and Glimcher, 1970; Lees, 1989). This differential rupture of the collagen molecule might explain the different microcrack pattern observed in the SOs of P-1 and UEK-1.

Generally, we could not identify any specific trend relating the depositional environment of the bone and its degree of micropreservation (see Table 2), which might suggest occasional transport and redeposition of bones. Well-preserved specimens of *Hipparion* and *Equus* (GHI = 4–5, see Fig. 5A, 5B) were recovered from either alluvial fan, lacustrine, or travertine sediments, while badly preserved metapodia (GHI = 0–2, see Fig. 5C–E) were found within fluvial and alluvial deposits (see Table 2). With the exception of Kırşehir-Kaman (Valli, 2005), taphonomy has not been properly studied yet for the different localities under analysis, and only some data about their lithology, stratigraphy, and/or sedimentary environments can be found in the literature (Tekkaya et al., 1975; Kaya, 1981; Forsten and Kaya, 1995; Kaya et al., 1998, 2005a, 2005b, 2012; Kazanci et al., 2005; Seyitoğlu et al., 2009; Mayda et al., 2013; Lebatard et al., 2014; Rausch et al., 2019). A complete taphonomical analysis would be useful to fully analyse the relationship between bone histology degradation and depositional environment, but this is beyond the scope of the present investigation. Thus, we encourage future research in this area.

CONCLUSIONS

Among the equid samples studied from Turkey, we found that a few had well-preserved histology, while the majority were diagenetically altered. In the specimens in which the histology was intact they compared favourably with European hipparionines, as well as with extant and extinct *Equus*. The *Hipparion* metatarsal (KK-1) permitted the identification of CCCB in the bone cortex, which is likely the result of the more distal location of the histological section on the bone shaft. Regarding vascularity, the proximal cross section of the P-1 *Equus* metacarpal showed a marked change in the orientation of the vascular canals within the mid-cortex that might be correlated with birth. The well-preserved bone histology and BGMs in MD-7 of *Cremohipparion* cf. *matthewi* permitted deductions concerning the later attainment of skeletal maturity as compared to other Mediterranean hipparionines.

The histology of most of the bones we studied was poorly preserved. Most of them were affected by non-Wedl tunnelling, suggesting that most of the *Hipparion* and *Equus* fossil metapodia analysed here were degraded by soil bacteria. Wedl-like tunnels were only recognized in KK-1, and their specific position and morphology agree with the damage caused by algae. Many of our specimens presented low histological preservation indexes (GHI = 0–2), so they likely experienced differences in moisture content during diagenesis. The well-preserved UEK-1, MD-7, and P-1 present higher preservation indices (GHI = 4–5) without signs of bioerosion, and we propose that they were initially buried in anoxic waterlogged conditions. UEK-1 and P-1 showed microcracks, which in the case of UEK-1 were likely formed in a water environment, and in P-1 (from the Pamukkale travertines) were most likely formed in response to intense heat and associated collagen denaturation. Given our small sample size, we did not identify a specific correlation between the degree of bone preservation and the sedimentary environment in which the different bones were found (i.e., alluvial fan, lacustrine, etc.).

Our analysis of the bone histology and the diagenetic alterations evident in the metapodia of late Miocene, Mio-Pleistocene, and early Pleistocene equids from Turkey provides a glimpse into the palaeobiology and early taphonomy of these extinct horses. Future research is encouraged to corroborate these initial findings. Furthermore, we note that histological research aiming at obtaining palaeobiological information should focus on the localities Manisa-Düzpınar and Uşak-Kemiklitepe 2 since bones from these sites presented excellent micropreservation. Indeed, increasing the sampling of *Cremohipparion* cf. *matthewi* from Manisa-Düzpınar would complement our interesting preliminary skeletochronological findings. Further taphonomical investigations at most of the fossil sites studied here will greatly enable a better understanding of bone preservation and the agents of bioerosion.

ACKNOWLEDGMENTS

We thank Petra Muller (University of Cape Town, South Africa) for guidance and assistance with SEM microscopy and Dr. Alberto Valenciano (Universidad de Zaragoza, Spain) for discussion and advice on several palaeontological aspects of the work. We are also grateful to the managing editor (Karin Perring), the senior editor (Prof. Nicholas Lancaster), the associate editor (Dr. Curtis W. Marean), and two anonymous reviewers, whose comments greatly improved an earlier version of this manuscript. Reviewer 1 is particularly acknowledged for suggesting that collagen thermal denaturation may be responsible for the microcracking observed in the SOs of P-1.

This work was supported by the Scientific and Technical Research Council of Turkey (TUBITAK), project number 110Y154, and the National Research Foundation (South Africa), grant number 117716 to AC. CN-M is supported by a postdoctoral research fellowship from the DST-NRF Centre of Excellence in Palaeosciences (CoE, South Africa), grants COE2019-PD03 and COEPD2020-39. Opinions expressed and conclusions arrived at are those of the authors and are not necessarily attributed to the CoE. SM and TK are grateful to Ege University Scientific Research Center for TTM/2016/002 and TTM/2013/001 research grants.

SUPPLEMENTARY MATERIAL

The supplementary material for this article can be found at https://doi.org/10.1017/qua.2020.87

REFERENCES

Akgün, F., Kayseri, M.S., Akkiraz, M.S., 2007. Palaeoclimatic evolution and vegetational changes during the Late Oligocene-Miocene period in Western and Central Anatolia (Turkey). *Palaeogeography, Palaeoclimatology, Palaeoecology* 253, 56–90.

Akkiraz, M.S., Akgün, F., Utescher, T., Bruch, A.A., Mosbrugger, V., 2011. Precipitation gradients during the Miocene in Western and Central Turkey as quantified from pollen data. *Palaeogeography, Palaeoclimatology, Palaeoecology* 304, 276–290.

Alberdi, M.T., 1989. A review of Old World hipparionine horses. In: Prothero, D.R., Schoch, R. (Eds.), *The Evolution of Perissodactyls*. Oxford University Press, New York, pp. 234–261.

Alberdi, M.T., Bonadonna, F.P., 1988. Equidae (Perissodactyla, Mammalia): extinctions subsequent to the climatic changes. *Revista Española de Paleontologia* 3, 39–43.

Alberdi, M.T., Cerdeño, E., 2003. Sistemática y distribución de los perisodáctilos del Neógeno y Cuaternario. In: Jiménez Fuentes, E., Civis Llovera, J. (Eds.), *Los Vertebrados Fósiles En La Historia de La Vida. Excavación, Estudio y Patrimonio*. Aquilafuente, Ediciones Universidad de Salamanca, Salamanca, pp. 237–279.

Alberdi, M.T., Ortiz-Jaureguizar, E., Prado, J.L., 1998. A quantitative review of European stenonoid horses. *Journal of Paleontology* 72, 371–387.

Alçiçek, M.C., Mayda, S., Alçiçek, H., 2012. Faunal and palaeoenvironmental changes in the Çal Basin, SW Anatolia: Implications for regional stratigraphic correlation of late Cenozoic basins. *Comptes Rendus - Geoscience* 344, 89–98.

Amprino, R., 1947. La structure du tissu osseux envisagée comme expression de différences dans la vitesse de l'accroissement. *Archives of Biology* 58, 315–330.

Amson, E., Kolb, C., Scheyer, T.M., Sánchez-Villagra, M.R., 2015. Growth and life history of Middle Miocene deer (Mammalia, Cervidae) based on bone histology. *Comptes Rendus - Palevol* 14, 637–645.

Antoine, P.-O., Saraç, G., 2005. Rhinocerotidae (Mammalia, Perissodactyla) from the late Miocene of Akkaşdağı, Turkey. *Geodiversitas* 27, 601–632.

Atalay, Z., 1980. Muğla-Yatağan ve Yakın Dolayı Karasal Neojen'inin Stratigrafi Araştırması. *Bulletin of the Geological Society of Turkey* 23, 3–99.

Azzaroli, A., 1992. Ascent and decline of monodactyl equids: a case for prehistoric overkill. *Annales Zoologici Fennici* 28, 151–163.

Bao, V., Rachel, H., Bradley, W., Curry Rogers, K., 2009. Patterns of microbial bioerosion in bones from the Campanian Judith River Formation of Montana. In: *Geological Society of America. Abstracts with Programs*. p. 628.

Bell, L.S., Skinner, M.F., Jones, S.J., 1996. The speed of post mortem change to the human skeleton and its taphonomic significance. *Forensic Science International* 82, 129–140.

Bernor, R.L., Göhlich, U.B., Harzhauser, M., Semprebon, G.M., 2017. The Pannonian C hipparions from the Vienna Basin. *Palaeogeography, Palaeoclimatology, Palaeoecology* 476, 28–41.

Bernor, R.L., Kovar-Eder, J., Lipscomb, D., Rögl, F., Sen, S., Tobien, H., 1988. Systematic, Stratigraphic, and Paleoenvironmental Contexts of First-Appearing Hipparion in the Vienna Basin, Austria. *Journal of Vertebrate Paleontology* 8, 427–452.

Bernor, R.L., Scott, R.S., Fortelius, M., Kappelman, J., Sen, S., 2003. Equidae (Perissodactyla). In: Fortelius, M., Kappelman, J., Sen, S., Bernor, R.L. (Eds.), *The Geology and Paleontology of the Miocene Sinap Formation, Turkey*. Columbia University Press, New York.

Bernor, R.L., Tobien, H., Woodburne, M.O., 1990. Patterns of Old World Hipparionine Evolutionary Diversification and Biogeographic Extension. In: Lindsay, E.H., Fahlbusch, V., Mein, P. (Eds.), *European Neogene Mammal Chronology*. Plenum Press, New York, pp. 263–319.

Bhat, M.S., Chinsamy, A., Parkington, J., 2019. Long bone histology of *Chersina angulata*: Interelement variation and life history data. *Journal of Morphology* 280, 1881–1899.

Bonar, L.C., Glimcher, M.J., 1970. Thermal denaturation of mineralized and demineralized bone collagens. *Journal of Ultrasructure Research* 32, 545–557.

Boulbes, N., Mayda, S., Titov, V.V., Alçiçek, M.C., 2014. Les grands mammifères du Villafranchien supérieur des travertins du Bassin de Denizli (Sud-Ouest Anatolie, Turquie). *Anthropologie*. 118, 44–73.

Boulbes, N., van Asperen, E.N., 2019. Biostratigraphy and Palaeoecology of European *Equus*. *Frontiers in Ecology and Evolution* 7, 301.

Brönnimann, D., Portmann, C., Pichler, S.L., Booth, T.J., Röder, B., Vach, W., Schibler, J., Rentzel, P., 2018. Contextualising the dead—Combining geoarchaeology and osteo-anthropology in a new multi-focus approach in bone histotaphonomy. *Journal of Archaeological Science* 98, 45–58.

Castanet, J., Croci, S., Aujard, F., Perret, M., Cubo, J., de Margerie, E., 2004. Lines of arrested growth in bone and age estimation in a small primate: *Microcebus murinus*. *Journal of Zoology* 263, 31–39.

Castanet, J., Francillon-Vieillot, H., Meunier, F., de Ricqlès, A., 1993. Bone and individual aging. In: Hall, B.K. (Ed.), *Bone: A Treatise*, Vol. 7. CRC Press, Boca Raton, pp. 245–283.

Child, A.M., 1995. Microbial taphonomy of archaeological bone. *Studies in Conservation* 40, 19–30.

Chinsamy-Turan, A., 2005. *The microstructure of dinosaur bone. Deciphering biology with fine-scale techniques*. The Johns Hopkins University Press, Baltimore and London.

Chinsamy-Turan, A., 2012. *Forerunners of mammals: radiation, histology, biology*. Indiana University Press, Bloomington.

Chinsamy-Turan, A., Ray, S., 2012. Bone histology of some Therocephalians and Gorgonopsians, and evidence of bone degradation by fungi. In: Chinsamy-Turan, A. (Ed.), *Forerunners of Mammals: Radiation, Histology, Biology*. Indiana University Press, Bloomington, pp. 199–222.

Chinsamy, A., Hanrahan, S.A., Neto, R.M., Seeley, M., 1995. A skeletochronological assessment of age in *Angolosaurus skoogi*, a lizard living in an aseasonal environment. *Journal of Herpetology* 29, 457–460.

Chinsamy, A., Raath, M.A., 1992. Preparation of fossil bone for histological examination. *Palaeontologia Africana* 29, 39–44.

Chinsamy, A., Valenzuela, N., 2008. Skeletochronology of the endangered side-neck turtles *Podocnemis expansa*. *South African Journal of Science* 104, 311–314.

Christol, J. de, 1832. Description d'*Hipparion*. *Annales des Sciences et de l'Industrie du Midi de France* 1, 180–181.

Currey, J.D., 2002. *Bones. Structure and mechanics*. Princeton University Press, Princeton.

Dal Sasso, G., Maritan, L., Usai, D., Angelini, I., Artioli, G., 2014. Bone diagenesis at the micro-scale: Bone alteration patterns during multiple burial phases at Al Khiday (Khartoum, Sudan) between the Early Holocene and the II century AD. *Palaeogeography, Palaeoclimatology, Palaeoecology* 416, 30–42.

Damann, F.E., Jans, M.M.E., 2017. Microbes, anthropology, and bones. In: Carte, D.O., Tomberlin, J.K., Benbow, M.E., Metcalf, J.L. (Eds.), *Forensic Microbiology*. John Wiley & Sons, Ltd, West Sussex, pp. 312–327.

Davis, P.G., 1997. The Bioerosion of Bird Bones. *International Journal of Osteoarchaeology* 7, 388–401.

https://doi.org/10.1017/qua.2020.87 Published online by Cambridge University Press

de Bonis, L., 2005. Carnivora (Mammalia) from the late Miocene of Akkaşdağı, Turkey. *Geodiversitas* 27, 567–589.

de Margerie, E., Cubo, J., Castanet, J., 2002. Bone typology and growth rate: Testing and quantifying "Amprino's rule" in the mallard (*Anas platyrhynchos*). *Comptes Rendus - Biology* 325, 221–230.

Demirel, F.A., Mayda, S., 2014. A new Early Pleistocene mammalian fauna from Burdur Basin, SW Turkey. *Russian Journal of Theriology* 13, 55–63.

de Ricqlès, A., 1975. Recherches paléohistologiques sur les os longs des tétrapodes VII.—Sur la classification, la signification fonctionnelle et l'histoire des tissus osseux des tétrapodes. Première partie, structures. *Annales de Paléontologie* (*Vertébrés*) 61, 51–129.

Eisenmann, V., Sondaar, P., 1998. Pliocene vertebrate locality of Çalta, Ankara, Turkey. 7. *Hipparion*. *Geodiversitas* 20, 409–439.

Enlow, D.H., 1962. A study of the post-natal growth and remodeling of bone. *American Journal of Anatomy* 110, 79–101.

Enlow, D.H., Brown, S.O., 1956. A comparative histological study of fossil and recent bone tissues. Part I. *Texas Journal of Science* 8, 405–412.

Enlow, D.H., Brown, S.O., 1957. A comparative histological study of fossil and recent bone tissues. Part II. *Texas Journal of Science* 9, 186–214.

Enlow, D.H., Brown, S.O., 1958. A comparative histological study of fossil and recent bone tissues. Part III. *Texas Journal of Science* 10, 187–230.

Erismis, U.C., Chinsamy, A., 2010. Ontogenetic Changes in the Epiphyseal Cartilage of *Rana* (*Pelophylax*) *caralitana* (Anura: Ranidae). *The Anatomical Record* 293, 1825–1837.

Erten, H., Sen, S., Özkul, M., 2005. Pleistocene mammals from travertine deposits of the Denizli basin (SW Turkey). *Annales du Paléontologie* 91, 267–278.

Fernández-Jalvo, Y., Andrews, P., 2016. *Atlas of Taphonomic Identifications. 1001+ Images of Fossil and Recent Mammal Bone Modification*, Vertebrate Paleobiology and Paleoantropology Series. Springer, Dordrecht.

Fernández-Jalvo, Y., Andrews, P., Pesquero, D., Smith, C., Marín-Monfort, D., Sánchez, B., Geigl, E.M., Alonso, A., 2010. Early bone diagenesis in temperate environments. Part I: Surface features and histology. *Palaeogeography, Palaeoclimatology, Palaeoecology* 288, 62–81.

Forsten, A., 1988. Middle Pleistocene replacement of stenonid horses by caballoid horses - Ecological implications. *Palaeogeography, Palaeoclimatology, Palaeoecology* 65, 23–33.

Forsten, A., 1989. Horse diversity through the ages. *Biological Reviews* 64, 279–304.

Forsten, A., Kaya, T., 1995. The hipparions (Mammalia, Equidae) from Gülpınar (Çanakkale, Turkey). *Paläontologische Zeitschrift* 69, 491–501.

Francillon-Vieillot, H., de Buffrénil, V., Castanet, J., Géraudie, J., Meunier, F.J., Sire, J.Y., Zylberberg, L., de Ricqlès, A., 1990. Microstructure and mineralization of vertebrate skeletal tissues. In: Carter, J.G. (Ed.), *Skeletal Biomineralization: Patterns, Processes and Evolutionary Trends*. Van Nostrand Reinhold, New York, pp. 471–530.

Galligani, P., Sartori, J., Barrientos, G., 2019. Bacterial bioerosion in human and animal bones from subtropical environments (Northern Pampa/Middle Paraná River Basin, República Argentina). *Journal of Archaeological Science: Reports* 25, 561–574.

Garcés, M., Cabrera, L., Agustí, J., Parés, J.M., 1997. Old world first appearance datum of "*Hipparion*" horses: Late Miocene large-mammal dispersal and global events. *Geology* 25, 19–22.

Garland, A.N., 1989. Microscopical analysis of fossil bone. *Applied Geochemistry* 4, 215–229.

Garrone, M.C., Cerda, I.A., Tomassini, R.L., 2019. Ontogenetic variability in the limb bones histology of plains vizcacha (*Lagostomus maximus*, Chinchillidae, Rodentia): implications for life history reconstruction of fossil representatives. *Historical Biology* In press.

Geiger, M., Wilson, L.A.B., Costeur, L., Sánchez, R., Sánchez-Villagra, M.R., 2013. Diversity and body size in giant caviomorphs (Rodentia) from the northern Neotropics - A study of femoral variation. *Journal of Vertebrate Paleontology* 33, 1449–1456.

Geraads, D., Gulec, E., Kaya, T., 2002. *Sinotragus* (Bovidae, mammalia) from Turkey and the Late Miocene Middle Asiatic Province. *Neues Jahrbuch für Geologie und Paläontologie Monatshefte* 8, 477–489.

Guo, L., Riding, R., 1998. Hot-spring travertine facies and sequences, Late Pleistocene, Rapolano Terme, Italy. *Sedimentology* 45, 163–180.

Hackett, C.J., 1981. Microscopical focal destruction (tunnels) in exhumed human bones. *Medicine, Science and the Law* 21, 243–265.

Hanson, M., Cain, C.R., 2007. Examining histology to identify burned bone. *Journal of Archaeological Science* 34, 1902–1913.

Haynes, S., Searle, J.B., Bretman, A., Dobney, K.M., 2002. Bone preservation and ancient DNA: The application of screening methods for predicting DNA survival. *Journal of Archaeological Science* 29, 585–592.

Hedges, R.E.M., 2002. Bone diagenesis: An overview of processes. *Archaeometry* 44, 319–328.

Hedges, R.E.M., Millard, A.R., Pike, A.W.G., 1995. Measurements and relationships of diagenetic alteration of bone from three archaeological sites. *Journal of Archaeological Science* 22, 201–209.

Hilgen, F.J., Lourens, L.J., Van Dam, J.A., Beu, A.G., Boyes, A.F., Cooper, R.A., Krijgsman, W., Ogg, James G., Piller, W.E., Wilson, D.S., 2012. The Neogene Period. In: Gradstein, F.., Ogg, J.G, Schmitz, M., Ogg, G. (Eds.), *The Geologic Time Scale*, Elsevier, Amsterdam, pp. 923–978.

Hollund, H.I., Jans, M.M.E., Collins, M.J., Kars, H., Joosten, I., Kars, S.M., 2012. What happened here? Bone histology as a tool in decoding the postmortem histories of archaeological bone from Castricum, The Netherlands. *International Journal of Osteoarchaeology* 22, 537–548.

Huttenlocker, A.K., Woodward, H.N., Hall, B.K., 2013. The biology of bone. In: Padian, K., Lamm, E.-T. (Eds.), *Bone Histology of Fossil Tetrapods: Advancing Methods, Analysis, and Interpretation*. University of California Press, Berkeley, pp. 13–34.

Jans, M.M.E., 2005. *Histological characterisation of diagenetic alteration of archaeological bone*. Vrije Universiteit, Amsterdam.

Jans, M.M.E., 2008. Microbial bioerosion of bone—a review. In: Wisshak, M., Tapanila, L. (Eds.), *Current Developments in Bioerosion*. Erlangen Earth Conference Series. Springer-Verlag, Berlin, Heidelberg, pp. 397–413.

Jans, M.M.E., Kars, H., Nielsen-Marsh, C.M., Smith, C.I., Nord, A.G., Arthur, P., Earl, N., 2002. *In situ* preservation of archaeological bone: a histological study within a multidisciplinary approach. *Archaeometry* 44, 343–352.

Jans, M.M.E., Nielsen-Marsh, C.M., Smith, C.I., Collins, M.J., Kars, H., 2004. Characterisation of microbial attack on archaeological bone. *Journal of Archaeological Science* 31, 87–95.

Jiménez-Moreno, G., Alçiçek, H., Alçiçek, M.C., van den Hoek Ostende, L., Wesselingh, F.P., 2015. Vegetation and climate

https://doi.org/10.1017/qua.2020.87 Published online by Cambridge University Press

changes during the late Pliocene and early Pleistocene in SW Anatolia, Turkey. *Quaternary Research* 84, 448–456.

Jordana, X., Marín-Moratalla, N., Moncunill-Solé, B., Nacarino-Meneses, C., Köhler, M., 2016. Ontogenetic changes in the histological features of zonal bone tissue of ruminants: a quantitative approach. *Comptes Rendus - Palevol* 15, 255–266.

Kahlke, R.D., García, N., Kostopoulos, D.S., Lacombat, F., Lister, A.M., Mazza, P.P.A., Spassov, N., Titov, V.V., 2011. Western Palaearctic palaeoenvironmental conditions during the Early and early Middle Pleistocene inferred from large mammal communities, and implications for hominin dispersal in Europe. *Quaternary Science Reviews* 30, 1368–1395.

Kaya, O., 1981. Miocene reference section for the coastal parts of West Anatolia. *Newsletters on Stratigraphy* 10, 164–191.

Kaya, O., Müller, E.D., Rückert-Ülkümen, N., Kaya, T., 1998. Biostratigraphic and Environmental Aspects of the Late Miocene-Early Pliocene Deposits in Develiköy (Manisa, Turkey). *Mitteilungen der Bayerischen Staatssammlung für Paläontologie und historische Geologie* 38, 3–7.

Kaya, T., Forsten, A., 1999. Late Miocene *Ceratotherium* and *Hipparion* (Mammalia, Perissodactyla) from Düzyayla (Hafik, Sivas), Turkey. *Geobios* 32, 743–748.

Kaya, T., Geraads, D., Tuna, V., 2005a. A new Late Miocene mammalian fauna in the Karaburun Peninsula (W Turkey). *Neues Jahrbuch für Geologie und Paläontologie - Abhandlungen Band* 236, 321–349.

Kaya, T., Mayda, S., Saraç, G., 2005b. A new Late Miocene mammalian fauna from Bayat (Kütahya, Western Turkey). In: *International Earth Sciences Colloquium on the Aegean Regions* (IESCA 2005). pp. 62–63.

Kaya, T.T., Mayda, S., Kostopoulos, D.S., Alcicek, M.C., Merceron, G., Tan, A., Karakutuk, S., Giesler, A.K., Scott, R.S., 2012. Şerefköy-2, a new Late Miocene mammal locality from the Yatağan Formation, Muğla, SW Turkey. *Comptes Rendus - Palevol* 11, 5–12.

Kayseri-Özer, M.S., Karadenizli, L., Akgün, F., Oyal, N., Saraç, G., Şen, Ş., Tunoğlu, C., Tuncer, A., 2017. Palaeoclimatic and palaeoenvironmental interpretations of the Late Oligocene, Late Miocene–Early Pliocene in the Çankırı-Çorum Basin. *Palaeogeography, Palaeoclimatology, Palaeoecology* 467, 16–36.

Kazanci, N., Karadenizli, L., Seyitoğlu, G., Sen, S., Alçiçek, M.C., Varol, B., Saraç, G., Hakyemez, Y., 2005. Stratigraphy and sedimentology of Neogene mammal bearing deposits in the Akkaşdağı area, Turkey. *Geodiversitas* 27, 527–551.

Kendall, C., Eriksen, A.M.H., Kontopoulos, I., Collins, M.J., Turner-Walker, G., 2018. Diagenesis of archaeological bone and tooth. *Palaeogeography, Palaeoclimatology, Palaeoecology* 491, 21–37.

Köhler, M., Marín-Moratalla, N., Jordana, X., Aanes, R., 2012. Seasonal bone growth and physiology in endotherms shed light on dinosaur physiology. *Nature* 487, 358–361.

Köhler, M., Moyà-Solà, S., 2009. Physiological and life history strategies of a fossil large mammal in a resource-limited environment. *Proceedings of the National Academy of Science of the United States of America* 106, 20354–20358.

Kolb, C., Scheyer, T.M., Lister, A.M., Azorit, C., de Vos, J., Schlingemann, M., Rössner, G.E., Monaghan, N.T., Sánchez-Villagra, M.R., 2015a. Growth in fossil and extant deer and implications for body size and life history evolution. *BMC Evolutionary Biology* 15, 19.

Kolb, C., Scheyer, T.M., Veitschegger, K., Forasiepi, A.M., Amson, E., Van der Geer, A.A.E., Van den Hoek Ostende, L.W., Hayashi, S., Sánchez-Villagra, M.R., 2015b. Mammalian bone palaeohistology: a survey and new data with emphasis on island forms. *PeerJ* 3, e1358.

Kontopoulos, I., Nystrom, P., White, L., 2016. Experimental taphonomy: post-mortem microstructural modifications in *Sus scrofa domesticus* bone. *Forensic Science International* 266, 320–328.

Kostopoulos, D.S., Saraç, G., 2005. Giraffidae (Mammalia, Artiodactyla) from the late Miocene of Akkaşdağı, Turkey. *Geodiversitas* 27, 735–745.

Kostopoulos, D.S., Sen, S., 1999. Late Pliocene (Villafranchian) mammals from Sarikol Tepe, Ankara, Turkey. *Mitteilungen der Bayerischen Staatssammlung für Paläontologie und historische Geologie* 39, 165–202.

Koufos, G.D., Kostopoulos, D.S., 1994. The late Miocene mammal localities of Kemiklitepe, Turkey: 3. Equidae. *Bulletin du Muséum National d'Histoire Naturelle* 16, 41–80.

Koufos, G.D., Mayda, S., Kaya, T., 2018. New carnivoran remains from the Late Miocene of Turkey. *PalZ* 92, 131–162.

Koufos, G.D., Vlachou, T.D., 2005. Equidae (Mammalia, Perissodactyla) from the late Miocene of Akkaşdağı, Turkey. *Geodiversitas* 27, 633–705.

Lebatard, A.E., Alçiçek, M.C., Rochette, P., Khatib, S., Vialet, A., Boulbes, N., Bourlès, D.L., *et al*., 2014. Dating the *Homo erectus* bearing travertine from Kocabaş (Denizli, Turkey) at at least 1.1 Ma. *Earth and Planetary Science Letters* 390, 8–18.

Lees, S., 1989. Some characteristics of mineralised collagen. In: Hukins, D.W.L. (Ed.), *Calcified Tissue*. The Macmillan Press, LTD, Houndmills, pp. 153–173.

Legendre, L.J., Botha-Brink, J., 2018. Digging the compromise: investigating the link between limb bone histology and fossoriality in the aardvark (*Orycteropus afer*). *PeerJ* 6, e5216.

Lindsay, E.H., Opdyke, N.D., Johnson, N.M., 1980. Pliocene dispersal of the horse *Equus* and late Cenozoic mammalian dispersal events. *Nature* 287, 135–138.

Liu, L., Kostopoulos, D.S., Fortelius, M., 2005. Suidae (Mammalia, Artiodactyla) from the late Miocene of Akkaşdağı, Turkey. *Geodiversitas* 27, 715–733.

Lyras, G.A., Giannakopoulou, A., Lillis, T., van der Geer, A.A.E., 2019. Paradise lost: Evidence for a devastating metabolic bone disease in an insular Pleistocene deer. *International Journal of Paleopathology* 24, 213–226.

Lyras, G.A., Giannakopoulou, A., Lillis, T., Veis, A., Papadopoulos, G.C., 2016. Bone lesions in a Late Pleistocene assemblage of the insular deer *Candiacervus* sp.II from Liko cave (Crete, Greece). *International Journal of Paleopathology* 14, 36–45.

MacFadden, B.J., 1984. Systematics and phylogeny of *Hipparion*, *Neohipparion*, *Nannippus*, and *Cormohipparion* (Mammalia, Equidae) from the Miocene and Pliocene of the New World. *Bulletin of the American Museum of Natural History* 179, 1–196.

MacFadden, B.J., 1985. Patterns of phylogeny and rates of evolution in fossil horses: hipparions from the Miocene and Pliocene of North America. *Paleobiology* 11, 245–257.

MacFadden, B.J., 1992. *Fossil horses. Systematics, Paleobiology, and Evolution of the Family Equidae*. Cambridge University Press, Cambridge.

MacFadden, B.J., 2005. Fossil Horses—Evidence for Evolution. *Science* 307, 1728–1730.

Marchiafava, V., Bonucci, E., Ascenzi, A., 1974. Fungal osteoclasia: a model of dead bone resorption. *Calcified Tissue Research* 14, 195–210.

https://doi.org/10.1017/qua.2020.87 Published online by Cambridge University Press

Marín-Moratalla, N., Jordana, X., García-Martínez, R., Köhler, M., 2011. Tracing the evolution of fitness components in fossil bovids under different selective regimes. *Comptes Rendus - Palevol* 10, 469–478.

Marín-Moratalla, N., Jordana, X., Köhler, M., 2013. Bone histology as an approach to providing data on certain key life history traits in mammals: implications for conservation biology. *Mammalian Biology* 78, 422–429.

Martínez-Maza, C., Alberdi, M.T., Nieto-Diaz, M., Prado, J.L., 2014. Life-history traits of the Miocene *Hipparion concudense* (Spain) inferred from bone histological structure. *PLoS One* 9, e103708.

Mayda, S., Sotnikova, M., Tesakov, A., Tan, A., Kaya, T., 2015. Miocene-Pliocene transitional mammalian fauna of Develi (Turkey). In: *61st Annual Session of the Russian Paleontologica Society*. April 13–17, 2015. Saint-Petersburg. Paleontological Society of the Russian Academy of Sciences. pp. 182–183.

Mayda, S., Titov, V.V., Tesakov, A., Göktaş, F., Alçiçek, M.C., 2013. Revision of Plio-Pleistocene mammalian faunas from Çobanisa area (Western Turkey). In: *VIII All-Russian Conference on Quaternary Research: Fundamental Problems of Queaternary, Results and Main Trands of Future Studies*. SSC RAS Publishers, Rostov-on-Don, p. 48.

Mayer, E.L., Hubbe, A., Botha-Brink, J., Ribeiro, A.M., Haddad-Martim, P.M., Neves, W., 2020. Diagenetic changes on bone histology of Quaternary mammals from a tropical cave deposit in southeastern Brazil. *Palaeogeography, Palaeoclimatology, Palaeoecology* 537, 109372.

McFarlin, S.C., Terranova, C.J., Zihlman, A.L., Enlow, D.H., Bromage, T.G., 2008. Regional variability in secondary remodeling within long bone cortices of catarrhine primates: The influence of bone growth history. *Journal of Anatomy* 213, 308–324.

Metcalf, J.L., Xu, Z.Z., Weiss, S., Lax, S., Treuren, W. Van, Hyde, E.R., Song, S.J., *et al*., 2016. Microbial community assembly and metabolic function during mammalian corpse decomposition. *Science* 351, 158–162.

Millard, A., 2001. The deterioration of bone. In: Brothwell, D.R., Pollard, A.M. (Eds.), *Handbook of Archaeological Sciences*. John Wiley & Sons, Ltd, Chichester, pp. 637–647.

Miszkiewicz, J.J., Louys, J., Beck, R.M.D., Mahoney, P., Aplin, K., O'Connor, S., 2020. Island rule and bone metabolism in fossil murines from Timor. *Biological Journal of the Linnean Society* 129, 570–586.

Miszkiewicz, J.J., Louys, J., O'Connor, S., 2019. Microanatomical record of cortical bone remodeling and high vascularity in a fossil giant rat midshaft femur. *The Anatomical Record* 302, 1934–1940.

Moncunill-Solé, B., Orlandi-Oliveras, G., Jordana, X., Rook, L., Köhler, M., 2016. First approach of the life history of *Prolagus apricenicus* (Ochotonidae, Lagomorpha) from Terre Rosse sites (Gargano, Italy) using body mass estimation and paleohistological analysis. *Comptes Rendus - Palevol* 15, 227–237.

Montoya-Sanhueza, G., Chinsamy, A., 2017. Long bone histology of the subterranean rodent *Bathyergus suillus* (Bathyergidae): ontogenetic pattern of cortical bone thickening. *Journal of Anatomy* 230, 203–233.

Morales, N.S., Catella, L., Oliva, F., Sarmiento, P.L., Barrientos, G., 2018. A SEM-based assessment of bioerosion in Late Holocene faunal bone assemblages from the southern Pampas of Argentina. *Journal of Archaeological Science: Reports* 18, 782–791.

Nacarino-Meneses, C., Jordana, X., Köhler, M., 2016a. Histological variability in the limb bones of the Asiatic wild ass and its significance for life history inferences. *PeerJ* 4, e2580.

Nacarino-Meneses, C., Jordana, X., Köhler, M., 2016b. First approach to bone histology and skeletochronology of *Equus hemionus*. *Comptes Rendus - Palevol* 15, 267–277.

Nacarino-Meneses, C., Köhler, M., 2018. Limb bone histology records birth in mammals. *PLoS One* 13, e0198511.

Nacarino-Meneses, C., Orlandi-Oliveras, G., 2019. The life history of European Middle Pleistocene equids: first insights from bone histology. *Historical Biology* In press.

Nielsen-Marsh, C., Gernaey, A., Turner-Walker, G., Hedges, R., Pike, A.W.G., Collins, M., 2000. The chemical degradation of bone. In: Cox, M., Mays, S. (Eds.), *Human Osteology: In Archaeology and Forensic Science*. Cambridge University Press, Cambridge, pp. 439–454.

Orlandi-Oliveras, G., Jordana, X., Moncunill-Solé, B., Köhler, M., 2016. Bone histology of the giant fossil dormouse *Hypnomys onicensis* (Gliridae, Rodentia) from Balearic Islands. *Comptes Rendus - Palevol* 15, 238–244.

Orlandi-Oliveras, G., Nacarino-Meneses, C., Koufos, G.D., Köhler, M., 2018. Bone histology provides insights into the life history mechanisms underlying dwarfing in hipparionins. *Scientific Reports* 8, 17203.

Orlando, L., 2015. Equids. *Current Biology* R973–R978.

Orlando, L., Ginolhac, A., Zhang, G., Froese, D., Albrechtsen, A., Stiller, M., Schubert, M., *et al*., 2013. Recalibrating *Equus* evolution using the genome sequence of an early Middle Pleistocene horse. *Nature* 499, 74–78.

Özkul, M., Kele, S., Gökgöz, A., Shen, C.C., Jones, B., Baykara, M.O., Fórizs, I., Németh, T., Chang, Y.W., Alçiçek, M.C., 2013. Comparison of the Quaternary travertine sites in the Denizli extensional basin based on their depositional and geochemical data. *Sedimentary Geology* 294, 179–204.

Pesquero, M.D., Bell, L.S., Fernández-Jalvo, Y., 2018. Skeletal modification by microorganisms and their environments. *Historical Biology* 30, 882–893.

Pfretzschner, H.-U., 2000. Microcracks and fossilization of Haversian bone. *Neues Jahrbbuch für Geologie und Paläontologie - Abhandlungen* 216, 413–432.

Pfretzschner, H.U., 2004. Fossilization of Haversian bone in aquatic environments. *Comptes Rendus - Palevol* 3, 605–616.

Pfretzschner, H.U., Tütken, T., 2011. Rolling bones—Taphonomy of Jurassic dinosaur bones inferred from diagenetic microcracks and mineral infillings. *Palaeogeography, Palaeoclimatology, Palaeoecology* 310, 117–123.

Prado, J.L., Alberdi, M.T., 1996. A cladistic analysis of the tribe Equini. *Palaeontology* 39, 663–680.

Pueyo, E.L., Muñoz, A., Laplana, C., Parés, J.M., 2016. The Last Appearance Datum of *Hipparion* in Western Europe: magnetostratigraphy along the Pliocene–Pleistocene boundary in the Villarroya Basin (Northern Spain). *International Journal of Earth Sciences* 105, 2203–2220.

Rausch, L., Alçiçek, H., Vialet, A., Boulbes, N., Mayda, S., Titov, V.V., Stoica, M., *et al*., 2019. An integrated reconstruction of the early Pleistocene palaeoenvironment of *Homo erectus* in the Denizli Basin (SW Turkey). *Geobios* 57, 77–95.

Rook, L., Bernor, R.L., Avilla, L.S., Cirilli, O., Flynn, L., Jukar, A., Sanders, W., Scott, E., Wang, X., 2019. Mammal Biochronology (Land Mammal Ages) Around the World From Late Miocene to Middle Pleistocene and Major Events in Horse Evolutionary History. *Frontiers in Ecology and Evolution* 7, 278.

Rook, L., Cirilli, O., Bernor, R.L., 2017. A Late Occurring "*Hipparion*" from the middle Villafranchian of Montopoli, Italy (early

https://doi.org/10.1017/qua.2020.87 Published online by Cambridge University Press

Pleistocene; MN16b; ca. 2.5 Ma). *Bolletino della Società Paleontologica Italiana* 56, 333–339.

Sander, P.M., Andrássy, P., 2006. Lines of arrested growth and long bone histology in Pleistocene large mammals from Germany: What do they tell us about dinosaur physiology? *Palaeontographica Abteilung A* 277, 143–159.

Saraç, G., Kaya, T., Geraads, D., 2002. *Ancylotherium pentelicum* (Perissodactyla, Mammalia) from the Upper Miocene of central and western Turkey. *Geobios* 35, 241–251.

Saraç, G., Sen, S., 2005. Chalicotheriidae (Mammalia, Perissodactyla) from the late Miocene of Akkaşdağı, Turkey. *Geodiversitas* 27, 591–600.

Schoeninger, M.J., Moore, K.M., Murray, M.L., Kingston, J.D., 1989. Detection of bone preservation in archaeological and fossil samples. *Applied Geochemistry* 4, 281–292.

Sen, S., 1990. *Hipparion* datum and its chronologic evidence in the Mediterranean area. In: Lindsay, E.H., Fahlbusch, V., Mein, P. (Eds.), *European Neogene Mammal Chronology*. Plenum Press, New York, pp. 495–505.

Sen, S., de Bonis, L., Dalfes, N., Geraads, D., Koufos, G.D., 1994. Les gisements de mammifères du Miocène supérieur de Kemiklitepe, Turquie: 1. Stratigraphie et magnétostratigraphie. *Bulletin du Muséum National d'Histoire Naturelle* 16, 5–17.

Sen, S., Seyitoğlu, G., Karadenizli, L., Kazanci, N., Varol, B., Araz, H., 1998. Mammalian biochronology of Neogene deposits and its correlation with the lithostratigraphy in the Çankırı-Çorum Basin, central Anatolia, Turkey. *Eclogae Geologicae Helvetiae* 91, 307–320.

Seyitoğlu, G., Alçiçek, C.M., Işık, V., Alçiçek, H., Mayda, S., Varol, B., Yılmaz, I., Esat, K., 2009. The stratigraphical position of Kemiklitepe fossil locality (Eşme, Uşsak) revised: Implications for the Late Cenozoic sedimentary basin development and extensional tectonics in western Turkey. *Neues Jahrbuch für Geologie und Paläontologie - Abhandlungen* 251, 1–15.

Strömberg, C.A.E., 2006. Evolution of hypsodonty in equids: testing a hypothesis of adaptation. *Paleobiology* 32, 236–258.

Tassy, P., 2005. Proboscideans (Mammalia) from the late Miocene of Akkaşdağı, Turkey. *Geodiversitas* 27, 707–714.

Tekkaya, I., Atalay, Z., Gürbüz, M., Ünay, E., Ermumcu, M., 1975. - Çankırı-Kalecik bölgesi karasal Neojeninin biostratigrafi araştırması. *Bulletin of the Geological Society of Turkey* 18, 77–80.

Tomassini, R.L., Miño-Boilini, Á.R., Zurita, A.E., Montalvo, C.I., Cesaretti, N., 2015. Modificaciones fosildiagenéticas en *Toxodon platensis* Owen, 1837 (Notoungulata, Toxodontidae) del Pleistoceno Tardío de la provincia de Corrientes, Argentina. Rev. Mex. *Ciencias Geológicas* 32, 283–292.

Trueman, C.N., Martill, D.M., 2002. The long-term survival of bone: the role of bioerosion. *Archaeometry* 44, 371–382.

Turner-Walker, G., 2012. Early bioerosion in skeletal tissues: Persistence through deep time. *Neues Jahrbuch für Geologie und Paläontologie - Abhandlungen* 265, 165–183.

Turner-Walker, G., 2019. Light at the end of the tunnels? The origins of microbial bioerosion in mineralised collagen. *Palaeogeography, Palaeoclimatology, Palaeoecology* 529, 24–38.

Turner-Walker, G., 2008. The chemical and microbial degradation of bones and teeth. In: Pinhasi, R., Mays, S. (Eds.), *Advances in Human Palaeopathology*. John Wiley & Sons, Ltd, Chichester, pp. 3–29.

Turner-Walker, G., Jans, M.M.E., 2008. Reconstructing taphonomic histories using histological analysis. *Palaeogeography, Palaeoclimatology, Palaeoecology* 266, 227–235.

Turner-Walker, G., Nielsen-Marsh, C.M., Syversen, U., Kars, H., Collins, M.J., 2002. Sub-micron Spongiform Porosity is the Major Ultra-structural Alteration Occurring in Archaeological Bone. *International Journal of Osteoarchaeology* 12, 407–414.

Valli, A.M.F., 2005. Taphonomy of the late Miocene mammal locality of Akkaşdağı, Turkey. *Geodiversitas* 27, 793–808.

van Asperen, E.N., 2012. Late Middle Pleistocene horse fossils from northwestern Europe as biostratigraphic indicators. *Journal of Archaeological Science* 39, 1974–1983.

van der Sluis, L.G., Hollund, H.I., Buckley, M., De Louw, P.G.B., Rijsdijk, K.F., Kars, H., 2014. Combining histology, stable isotope analysis and ZooMS collagen fingerprinting to investigate the taphonomic history and dietary behaviour of extinct giant tortoises from the Mare aux Songes deposit on Mauritius. *Palaeogeography, Palaeoclimatology, Palaeoecology* 416, 80–91.

Veitschegger, K., Kolb, C., Amson, E., Scheyer, T.M., Sánchez-Villagra, M.R., 2018. Palaeohistology and life history evolution in cave bears, *Ursus spelaeus* sensu lato. *PLoS One* 13, e0206791.

Walker, M.M., Louys, J., Herries, A.I.R., Price, G.J., Miszkiewicz, J.J., 2020. Humerus midshaft histology in a modern and fossil wombat. *Australian Mammalogy* In press.

White, L., Booth, T.J., 2014. The origin of bacteria responsible for bioerosion to the internal bone microstructure: Results from experimentally-deposited pig carcasses. *Forensic Science International* 239, 92–102.

Woodburne, M.O., Bernor, R.L., 1980. On Superspecific Groups of Some Old World Hipparionine Horses. *Journal of Paleontology* 54, 1319–1348.

Woodward, H.N., Padian, K., Lee, A.H., 2013. Skeletochronology. In: Padian, K., Lamm, E.-T. (Eds.), *Bone Histology of Fossil Tetrapods: Advancing Methods, Analysis, and Interpretation*. University of California Press, Berkeley, pp. 195–215.

Woolley, M.R., Chinsamy, A., Govender, R., Bester, M.N., 2019. Microanatomy and histology of bone pathologies of extant and extinct phocid seals. *Historical Biology* In press.

Zedda, M., Sathe, V., Chakraborty, P., Palombo, M.R., Farina, V., 2020. A first comparison of bone histomorphometry in extant domestic horses (*Equus caballus* Linnaeus, 1758) and a Pleistocene Indian wild horse (*Equus namadicus* Falconer & Cautley, 1849). *Integrative Zoology* In press.

https://doi.org/10.1017/qua.2020.87 Published online by Cambridge University Press